International Journal of Heat and Mass Transfer 150 (2020) 119312

Contents lists available at ScienceDirect

International Journal of Heat and Mass Transfer

journal homepage: www.elsevier.com/locate/hmt

Experimental investigation on loop thermosyphon thermal performance with flow visualization

Sara Kloczko*, Amir Faghri

Department of Mechanical Engineering, University of Connecticut, 191 Auditorium Road, Storrs, CT 06269-3139, USA

ARTICLE INFO

Article history:
Received 29 September 2019
Revised 15 December 2019
Accepted 3 January 2020
Available online 23 January 2020

ABSTRACT

A non-phase change heat pipe (NPCHP) with no wick was proposed as a new heat pipe which is not dependent on a wick or phase change at steady state operation and where the heat transfer is driven by the pressure response to a heat input, rather than phase change. It was shown recently that the NPCHP is not a new heat pipe as suggested but is a loop thermosyphon (Kloczko et al., 2019). This effort focuses on understanding how changing different system parameters, including heat input, fill ratio, inclination angle, and working fluid affects the overall system performance of both the single-phase and two-phase loop thermosyphons. Flow visualization is incorporated and the flow of liquid/vapor through the thermosyphon is studied. Depending upon the initial fill ratio of the loop thermosyphon and the working fluid, the thermosyphon is shown to either operate as a two-phase loop thermosyphon or a single-phase loop thermosyphon.

1. Introduction

A heat pipe is a highly effective and well-established device which transfers a large amount of heat from one location to another. The components of a conventional heat pipe are the wick, outer wall, and working fluid, which flows through the three main sections of the heat pipe: evaporator, adiabatic section, and condenser [9]. A diagram of a conventional heat pipe is shown in Fig. 1a [3]. There is a small temperature drop between the evaporator and condenser section of the heat pipe, referred to as the adiabatic section, where the heat pipe operates nearly isothermally [10]. Heat is applied externally to the evaporator section and vaporizes the fluid in the saturated wick, which is driven by the vapor pressure through the adiabatic section to the condenser where it condenses and releases its latent heat, then is returned to the evaporator by capillary action of the wick [7,24]. The main driver of heat transfer in the conventional heat pipe is phase change and the wick. There are several different types of heat pipe depending on the application, including: conventional heat pipes, loop heat pipes (LHP), pulsating heat pipes (PHP), and thermosyphons, which can also be broken up into conventional thermosyphons and single- and two-phase loop thermosyphons. A conventional heat pipe reliant on phase change has several limits. These limits include the viscous, sonic, capillary, entrainment, flooding, and boiling limits. Challenges and opportunities of heat pipes are discussed by Faghri [8]. Heat pipe analysis and numerical simulation covering all types of heat pipes with various levels of approximation is reviewed by Bergman & Faghri [2].

A two-phase conventional thermosyphon (TPCTS), a schematic of which is shown in Fig. 1b, is sometimes referred to as a gravity assisted heat pipe and consists of an evaporator and condenser. There is no wick in a TPCTS because the force of gravity drives the fluid flow. The liquid and vapor occupy a single straight tube and the flow is counter-current. The heat input to the evaporator vaporizes the working fluid, which then flows up to the condenser. The working fluid is then condensed back into a liquid, releases its latent heat, and drains back down the walls to the evaporator.

Due to the counter-current flow of the liquid and vapor, the thermosyphon performance is limited by the flooding limit. This occurs when working fluid temperature is low, and vapor velocity is high. The shear of the vapor traveling to the condenser prevents liquid film on the wall from traveling back to the condenser. The conventional thermosyphon is also subject to the dry-out limit. This occurs when the fill ratio is too small and the condensate film eventually dries out [22]. Thermosyphon performance has been studied extensively, varying several parameters including: working fluid, fill ratio, heat input, and orientation. For conventional thermosyphons, fill ratio is usually described as volume of working fluid relative to the volume of the evaporator. The fill ratio is sometimes also reported as volume of working fluid relative to the total thermosyphon volume. For the experiment discussed, fill ratio is the percentage of volume filled with respect to the total volume of the loop. Smith et al. (2016) tested several fill ratios between

* Corresponding author.

https://doi.org/10.1016/j.ijheatmasstransfer.2020.119312
0017-9310/

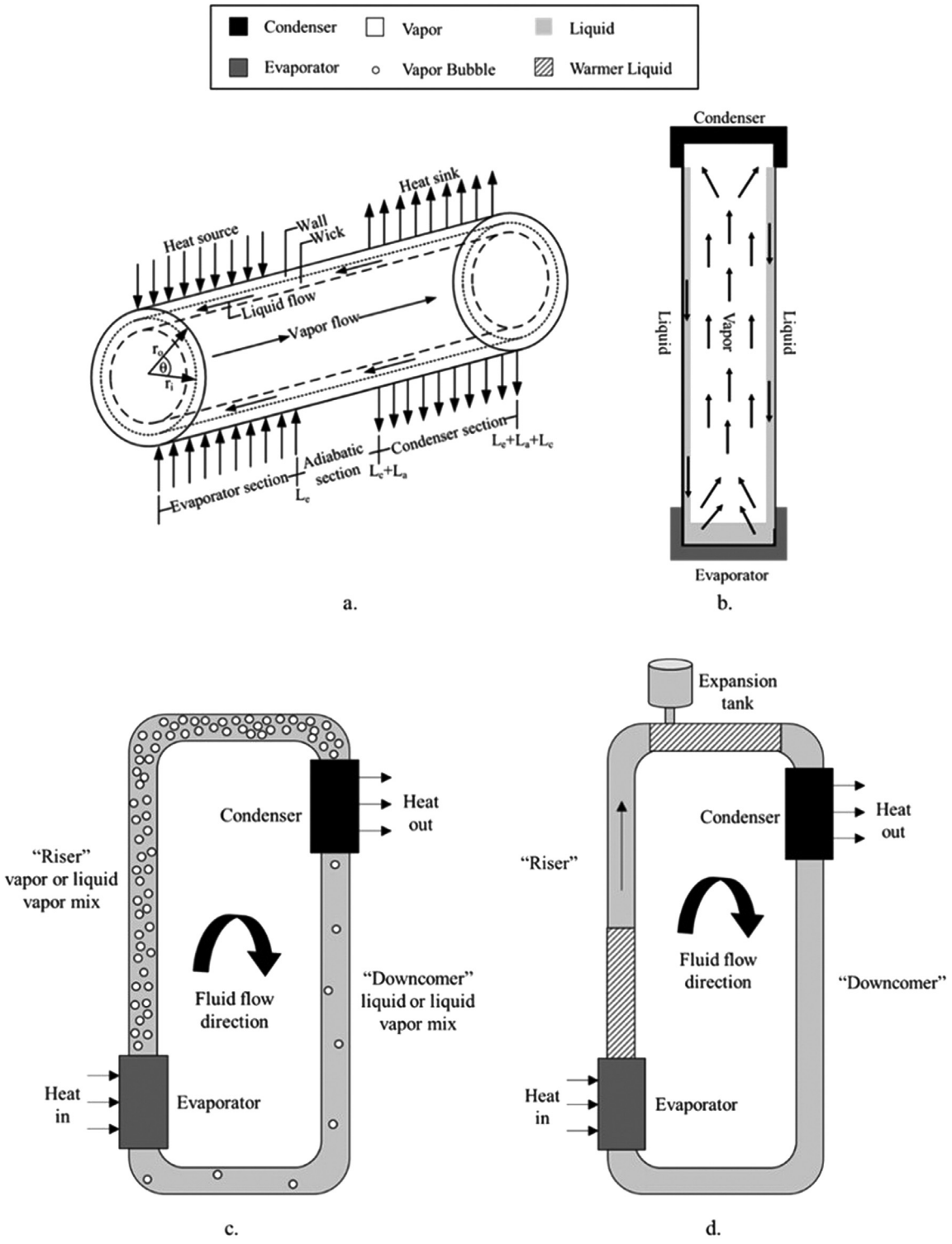

Fig. 1. Diagrams of a. Conventional heat pipe b. Two-phase conventional thermosyphon c. Two-phase loop thermosyphon d. Single-phase loop thermosyphon showing the flow of liquid and/or vapor.

50% and 150% of the evaporator volume and reported the optimal fill ratio to be 100% (the evaporator is initially entirely filled with working fluid), in their case water was used.

The two-phase loop thermosyphon (TPLTS), a general schematic of which is shown in Fig. 1c, consists of an evaporator, riser, condenser, and downcomer. Heat input to the evaporator section vaporizes the working fluid [27]. The vapor (or liquid-vapor mix, depending on the initial fill ratio) then flows up the riser to the condenser where it is condensed back into a liquid. The flow in the TPLTS is co-current, with liquid and vapor flowing in the same direction around the loop. The liquid phase (or liquid-vapor mix, depending on the initial fill ratio) flows down the downcomer back to the evaporator. The flow of liquid is driven by the density difference of the lower temperature fluid coming from the condenser

and the higher temperature lower density flow from the evaporator [14]. The TPLTS has no flooding limit. Some TPLTS have wicks in the evaporator and some do not. However, the TPLTS operates more effectively with wick structures in the evaporator than without [13]. The TPLTS relies on gravity for the flow of working fluid, and the heat transfer relies on the heat of vaporization.

Several key parameters that influence the performance of the TPLTS are: heat input, internal tube diameter, distance between evaporator and condenser, length of heat input zone, thermo physical properties of working fluid, operating pressure, and fill ratio [11]. For low fill ratios, there is no liquid in the riser (section through which vapor flows to the evaporator), and for high fill ratios, generally greater than 100% relative to the evaporator volume, there is a mixture of liquid and vapor in both the riser and the downcomer (section connecting the condenser to the evaporator through which the condensed working fluid flows) [25]. The TPLTS relies on gravity for the flow of working fluid, and the heat transfer relies on the heat of vaporization.

The ideal fill ratio depends on the boiling point and latent heat of the fluid being used. For low fill ratios, dry-out may occur for systems with wick structures [13]. The amount of working fluid is chosen such that the liquid builds up in the downcomer below the condenser, thus generating hydrostatic head in the evaporator. When water is used as the working fluid, optimal fill ratios of 30% were reported by Kang et al. [13], Chehade et al. [5] determined the optimal fill ratio to be between 7% and 10% relative to the total loop volume, and Chang et al. [4] reported an optimal fill ratio of 50% relative to the evaporator volume. Several other working fluids have been tested in TPLTS and optimal fill ratios were determined. According to Kang et al., [13] the ideal fill ratio is 10% with methanol as the working fluid. Naresh & Balaji [20] concluded the optimal volume of R134a as the working fluid is 50% relative to the volume of the evaporator. Park et al. [22] studied a TPLTS with FC-72 as the working fluid, and concluded that a 10% fill ratio resulted in dry-out, and a 50% fill ratio resulted in flooding, therefore the optimal fill ratio is between those two values. Fu et al. [12] reported the fill ratio should be between 30–80% of the total loop volume with ammonia as the working fluid. Values less than 30% resulted in dry-out and values greater than 80% resulted in flooding. Beitelmal & Patel [1] report optimal charge amounts to be between 10% and 15% PF-5060 relative to the total volume available in the evaporation chamber. Based on the literature review discussed above, it is clear the optimal fill ratio varies greatly depending on the working fluid and other system parameters, including size of the evaporator relative to the remainder of the loop.

The third type of thermosyphon is the single-phase loop thermosyphon (SPLTS) which is also sometimes referred to as single-phase natural circulation loop, a general schematic of which is shown in Fig. 1d. The basic structure is the same as that of a TPLTS where there is an evaporator section that heats the working fluid, a pipe connects the evaporator to the condenser (riser), the condenser cools the working fluid, and another pipe connects the condenser to the evaporator (downcomer) through which the working fluid flows back to the evaporator. The flow is driven by the hydrostatic pressure difference that results from the temperature gradient and resulting density gradient from the evaporator to the condenser. Fluid motion is generated by density differences in the working fluid due to temperature gradients generated by the evaporator and condenser [18]. The motion is governed by the balance of the opposite effects of buoyancy (due to the different fluid densities in the ascending (warm) and descending (cold) sections), and friction [19]. Generally, the heat sink is above the heat source to enhance the circulation rates [26]. A disadvantage of the SPLTS is that interaction between buoyancy and frictional forces can be unstable. There is also an expansion tank shown in Fig. 1d which may be present in a SPLTS to accommodate the volume expansion of working fluid as temperature increases.

The SPLTS studied by Dobson & Ruppersberg [6] has an expansion tank into which excess fluid flows as a result of thermal expansion. The expansion tank serves to ensure the pressure in the tank does not get too high. Pilkhwal et al. [23] also used an expansion tank in their experiment to allow for the expansion of working fluid (in this case water). Naveen et al. [21] explain the expansion tank is necessary to vent the air out during the loop filling, and to accommodate the swells and shrinkages of the fluid within the loop during transient operation. Typically, the SPLTS is fully filled with liquid working fluid.

The NPCHP was proposed by Lee et al. [[16,17]b] as a new heat pipe. However, it was shown in a previous effort by the present authors [15] that the NPCHP is a loop thermosyphon and can operate as either a single- or two-phase loop thermosyphon depending on liquid fill ratio and working fluid. The purpose of this effort is to perform a detailed experimental analysis with the goal of determining effects of heat input, fill ratio, working fluid, and inclination angle on the thermal performance in loop thermosyphons. These results will be used to determine the optimal operating conditions for this device. Flow visualization is incorporated to study how changing the system parameters mentioned previously affects the liquid/vapor flow through the loop.

2. Experiment setup

The loop thermosyphon experiment consists of a loop of stainless-steel pipe filled with working fluid. Experiments are run using two different working fluids, water and R134a. The amount of working fluid in the system is varied between 25–100% relative to total loop volume. A diagram of the experiment is shown in Fig. 2. The evaporator section (1) consists of three AC 110 V 100–300 W 2 Wire Mold Cartridge Heater Pipe Heating Elements (12 mm × 80 mm). A pressure release valve (2) is added to release pressure from the system if it increases above 350 psi. Fluid release and fill valves (3) are used to add and remove working fluid from the system and adjust fill ratio. The condenser section of the loop thermosyphon consists of a cooling jacket (4) surrounding a section of the pipe. Cold water (5 °C), which is cooled by two LAUDA Alpha RA8 water coolers (5), flows through the cooling jacket. Heat is transferred out of the system into the cooling water. The flowmeter (FL-3440ST) (6) is used to adjust the flow rate of the cooling water moving through the cooling jacket. The variable automatic transformer (Staco Energy Products Co 3PN1510) (7) adjusts the power supplied to the heating element. The digital wattmeter (Vector-Vid WD-767) (8) reads the value of power supplied to the heating element.

The entire pipe is insulated with one layer of 1in thick ceramic fiber insulation. The heating element is surrounded by three layers of insulation. The pipe material is stainless steel with outer and inner diameters of 12.7 mm and 10.9 mm, respectively. The overall height and width of the pipe are 1.465 m and 0.395 m, respectively. There are three flow visualization windows at different locations around the loop as shown in Fig. 2. One flow visualization window is located just after the heating element, labeled “window 1″ to view bubble formation. The second window is located at the top right of the loop, labeled “window 2″. This window is used to determine if the working fluid is circulating. The third window is located after the condenser and shows the phase of the working fluid just after the coldest portion of the loop, labeled “window 3″. The flow visualization windows consist of 5in long borosilicate glass tubes fitted to the stainless steel pipe using Swagelok fittings with PTFE ferrules and are supported by a piece of aluminum to avoid bending of the glass. A schematic of the flow visualization windows is shown in Fig. 3. The flow is cir-

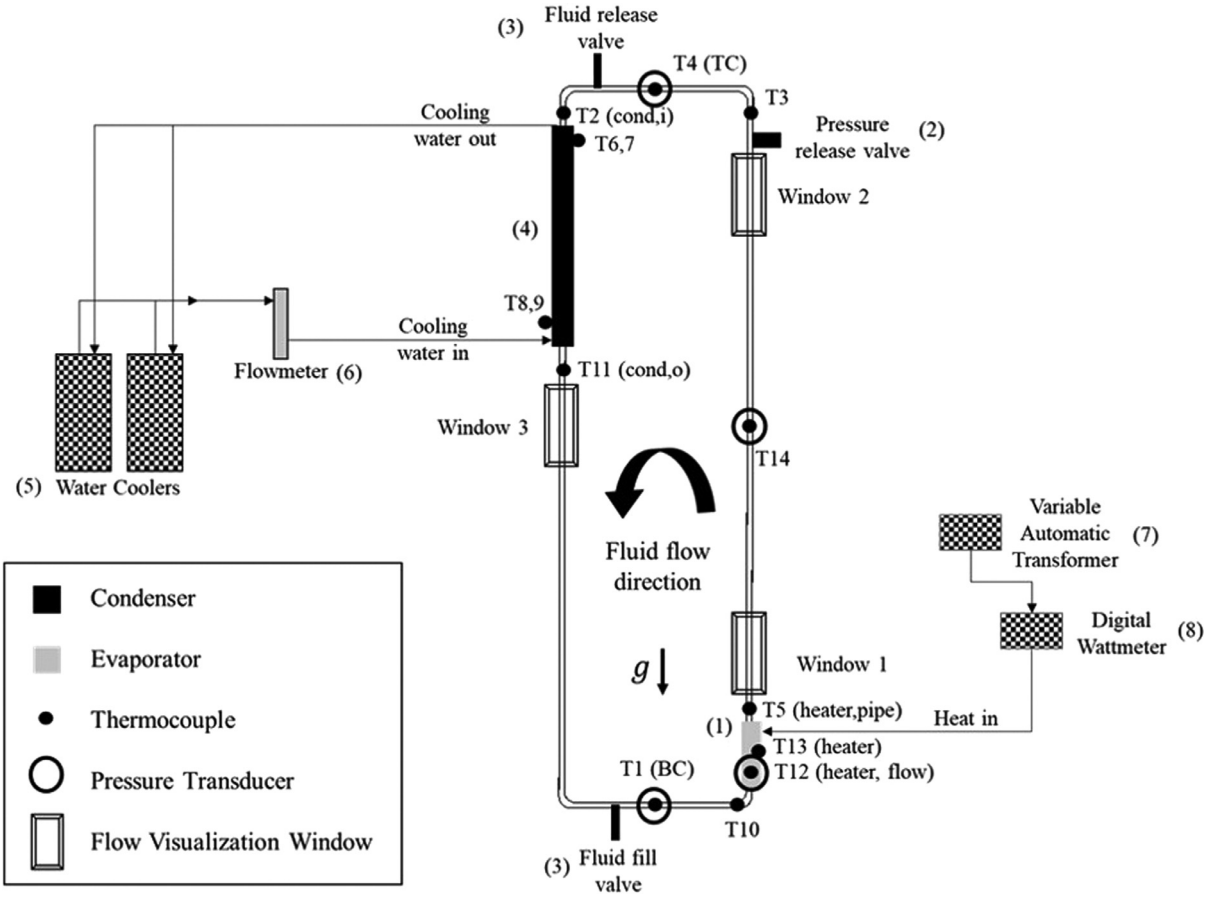

Fig. 2. Loop thermosyphon experimental setup.

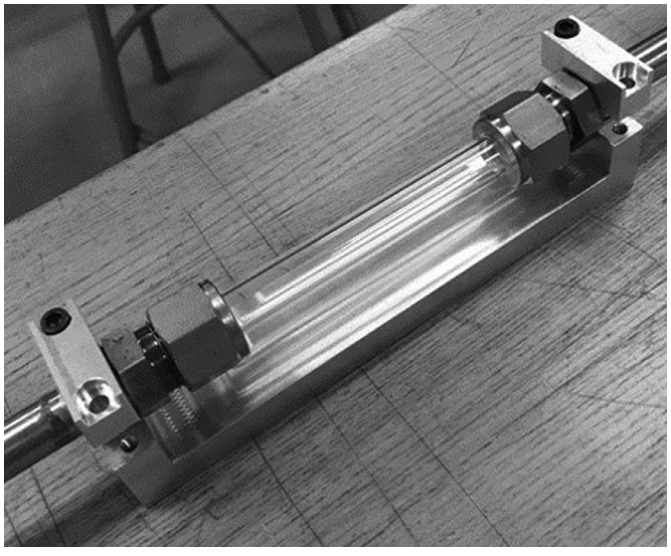

Fig. 3. Flow visualization window.

culating counter-clockwise around the loop and gravity is acting in the direction indicated in Fig. 2.

K-type thermocouples and pressure transducers (Digi-Key P51-500-A-A-I36-5V-000-000 500 Psia 1/4NPT 5 V) are placed at multiple locations around the loop. Instrumentation locations are shown in Fig. 2. The temperatures just before and after the heating element and just above and below the condenser, cond,i and cond,o respectively, are used to calculate the thermal conductivity and thermal resistance of the system. Thermal response time of the system to a heat input can be observed by plotting temperatures at various locations with time.

Thermocouples T1-5, T10, T11, and T14 are placed on the outside of the pipe. T10 measures the temperature just before the evaporator, T5 is the temperature just after the evaporator, T4 is the top center (TC) temperature, T2 and T11 are the temperatures before and after the condenser, respectively, and T1 is the bottom center (BC) temperature. T8-9 and T6-7 are the cooling water inlet and outlet temperatures, respectively. T12 measures the temperature of the working fluid inside the pipe. T13 measures the temperature of the heating element.

The uncertainty in the pressure transducers is ±0.5%. The uncertainty in the temperatures recorded by the K-type thermocouples is determined by calibrating the thermocouples with constant temperature baths. The thermocouple uncertainty is calculated to be ±0.42 K. Uncertainty in heat input is ±1 W. The equation for thermal resistance was used to perform error propagation and the calculated error values in thermal resistance at heat inputs of 100, 150, 200, 250, 300, and 350 W are approximately ±0.0063, 0.0037, 0.0026, 0.0021, 0.0017, and 0.0015 K/W, respectively. These values vary slightly for each experiment depending on fill ratio and working fluid.

3. Effects of changing fill ratio

Two different working fluids are used, R134a and water. All fill ratio experiments are conducted with the experiment oriented vertically with the evaporator located below the condenser on opposite sides of the loop (as shown in Fig. 2).

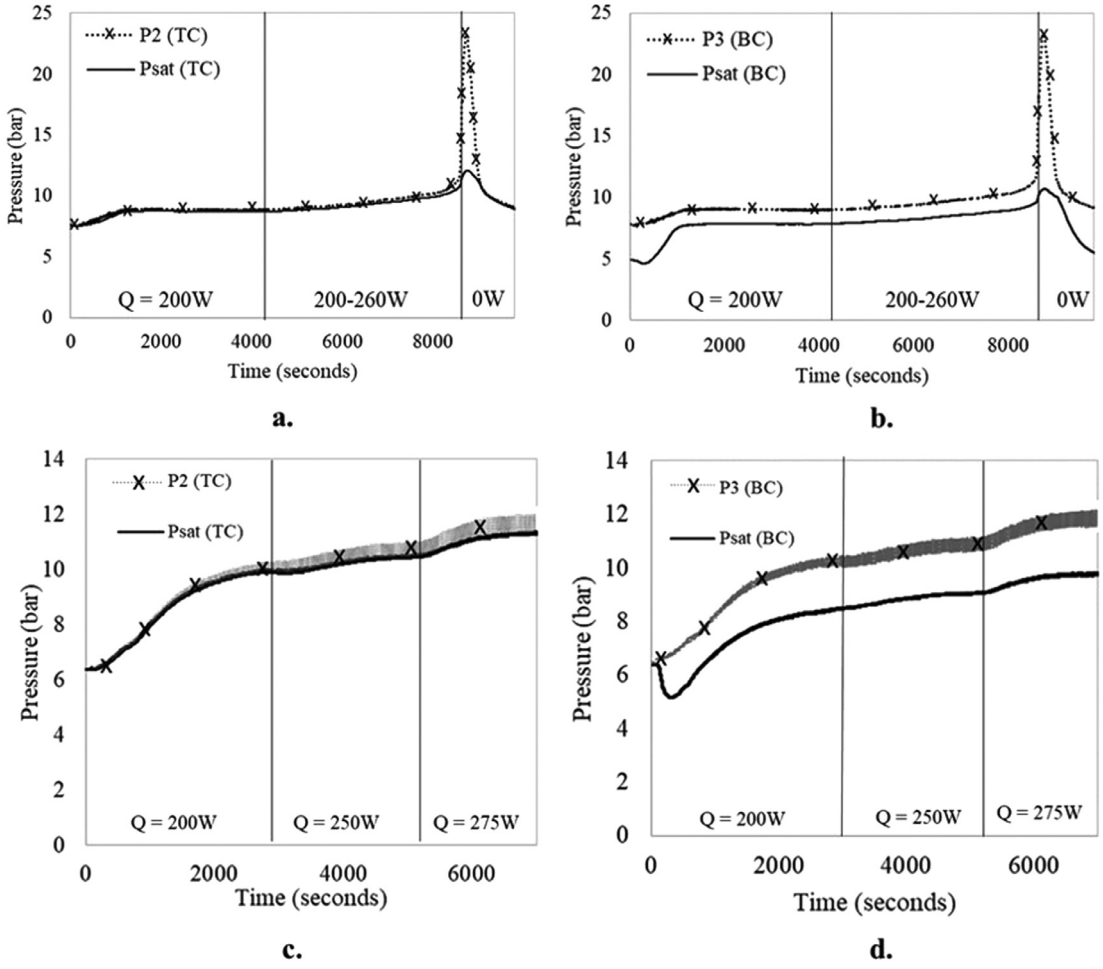

Fig. 4. Experimental pressure response to heat input for a loop thermosyphon at a. TC (95% R134a, 200–260 W), b. BC (95% R134a, 200–260 W), c. TC (90% R134a, 200–275 W), d. BC (90% R134a, 200–275 W).

3.1. Effect of changing fill ratio with R134a as the working fluid

Fill ratios of 100–25% of the total loop volume have been tested, while removing R134a in increments of approximately 5%. The 100% fill ratio is run with a 200 W heat input and reached the maximum allowable temperature quickly. Therefore, results are not shown. Results for thermal resistance and experimental trends are summarized in Table 1. The 95% is the only fill ratio experiment with R134a as the working fluid where the system reached the fully filled condition. This occurs when the working fluid temperature increases enough such that the liquid expands to fill the entire pipe. This is determined by the large spike in pressure, as shown in Fig. 4a and 4b, and the lack of vapor bubbles in the flow visualization windows.

As seen in Fig. 4a and 4b, there is a very small amount of time during which the pressure begins to increase steeply. As soon as this trend is noticed, the heating element is shut off so as not to exceed the maximum pressure and damage the experiment. This significant pressure rise is a result of the system becoming fully filled with liquid. It can be seen in Fig. 4a that the pressure, after about 8000 s, begins to rise above the saturation pressure at the TC location. This indicates the working fluid is in the compressed liquid phase. When the fully filled state is reached, volume expansion is limited. Therefore, any additional increase in temperature is accompanied by a rapid rise in pressure, as shown in Fig. 4a and 4b.

Experimental data for the 90% fill ratio is shown in Fig. 4c and 4d. As seen in Fig. 4c, while there is fluctuation in the system pressure, the system pressure does not noticeably exceed the saturation pressure at the TC location. This, along with the observation that there are still vapor bubbles in the flow visualization windows throughout the experiment, shows the 90% fill ratio experiment does not reach the fully filled condition and operates as two-phase for heat inputs up to 275 W with R134a as the working fluid.

Similar trends are observed for the 85–25% fill ratio experiments. The maximum amount of heat the system is able to transfer without exceeding maximum system temperature and pressure varies by fill ratio and is listed in Table 1. The experiment with initial fill ratio of 30% is able to reach steady state for heat inputs up to 250 W. After the 300 W input is applied to the 30% fill ratio experiment, the temperature just after the heating element begins to rise rapidly and the heating element is shut off to prevent the system from surpassing the maximum allowable temperature. Results from the 30% fill ratio experiment are shown in Fig. 5. The 25% fill ratio experiment is not able to reach steady state for a heat input of 200 W. The same trend that is seen in Fig. 5 where the temperature just after the heating element increases very rapidly is seen, which indicates the fill ratio of 25% is too low to transfer 200 W of heat from the heating element to the condenser.

It can be concluded that, with the current experimental conditions and parameters, only the 95% R134a fill ratio experiment reached the fully filled condition where all the working fluid is

Table 1
Effects of R134a fill ratio (% relative to total loop volume) on experimental performance of a loop thermosyphon.

Fill ratio		200 W	250 W	300 W	325 W
95%	Single- or Two-phase?	Two-phase	Single-Phase	Maximum allowable temperature reached.	Maximum allowable temperature reached.
	Pulsation?	No	No	N/A	N/A
	Vapor After Condenser?	No	No	N/A	N/A
	Operate as Heat Pipe?	TPLTS	No	N/A	N/A
	Thermal Resistance (K/W)	0.017	N/A	N/A	N/A
	Comments	N/A	N/A	N/A	N/A
90%	Single- or Two-phase?	Two-phase	Two-phase	Two-phase	Maximum allowable temperature reached.
	Pulsation?	Yes	Yes	Yes	N/A
	Vapor After Condenser?	No	No	No	N/A
	Operate as Heat Pipe?	TPLTS	TPLTS	TPLTS	N/A
	Thermal Resistance (K/W)	0.026	0.020	0.021	N/A
	Comments	N/A	N/A	N/A	N/A
85%	Single- or Two-phase?	Two-phase	Two-phase	Two-phase	Maximum allowable temperature reached.
	Pulsation?	Yes	Yes	Yes	N/A
	Vapor After Condenser?	No	Yes	Yes	N/A
	Operate as Heat Pipe?	TPLTS	TPLTS	TPLTS	N/A
	Thermal Resistance (K/W)	0.022	0.019	0.021	N/A
	Comments	N/A	N/A	N/A	N/A
80%	Single- or Two-phase?	Two-phase	Two-phase	Two-phase	Maximum allowable temperature reached.
	Pulsation?	Yes	Yes	Yes	N/A
	Vapor After Condenser?	Yes	Yes	Yes	N/A
	Operate as Heat Pipe?	TPLTS	TPLTS	TPLTS	N/A
	Thermal Resistance (K/W)	0.017	0.018	0.019	N/A
	Comments	N/A	N/A	N/A	N/A
75%	Single- or Two-phase?	Two-phase	Two-phase	Two-phase	Two-phase
	Pulsation?	No	No	No	No
	Vapor After Condenser?	No	Yes	Yes	Yes
	Operate as Heat Pipe?	TPLTS	TPLTS	TPLTS	TPLTS
	Thermal Resistance (K/W)	0.017	0.018	0.019	0.020
	Comments	N/A	N/A	N/A	N/A
70%	Single- or Two-phase?	Two-phase	Two-phase	Two-phase	Two-phase
	Pulsation?	No	No	No	No
	Vapor After Condenser?	No	No	No	No
	Operate as Heat Pipe?	TPLTS	TPLTS	TPLTS	TPLTS
	Thermal Resistance (K/W)	0.020	0.021	0.022	0.023
	Comments	N/A	N/A	N/A	N/A
65%	Single- or Two-phase?	Two-phase	Two-phase	Two-phase	Maximum allowable temperature reached.
	Pulsation?	No	No	No	N/A
	Vapor After Condenser?	Yes	Yes	Yes	N/A
	Operate as Heat Pipe?	TPLTS	TPLTS	TPLTS	N/A
	Thermal Resistance (K/W)	0.018	0.020	0.022	N/A
	Comments	N/A	N/A	N/A	N/A
60%	Single- or Two-phase?	Two-phase	Two-phase	Two-phase	Maximum allowable temperature reached.
	Pulsation?	No	No	No	N/A
	Vapor After Condenser?	Yes	Yes	Yes	N/A
	Operate as Heat Pipe?	TPLTS	TPLTS	TPLTS	N/A
	Thermal Resistance (K/W)	0.018	0.018	0.021	N/A
	Comments	Liquid-vapor interface visible in window 3 – liquid level fluctuates slightly as liquid drains down pipe wallLiquid level in window 3 gets lower with increasing heat input			
55%	Single- or Two-phase?	Two-phase	Two-phase	Two-phase	Maximum allowable temperature reached.
	Pulsation?	No	No	No	N/A
	Vapor After Condenser?	Yes	Yes	Yes	N/A
	Operate as Heat Pipe?	TPLTS	TPLTS	TPLTS	N/A
	Thermal Resistance (K/W)	0.024	0.025	0.025	N/A
	Comments	Amount/speed of liquid draining down walls of window 3 increases with increasing heat inputLiquid did not appear in window 2 until the end of the 200 W heat input segment of the experiment			
50%	Single- or Two-phase?	Two-phase	Two-phase	Two-phase	Maximum allowable temperature reached.
	Pulsation?	No	No	No	N/A
	Vapor After Condenser?	Yes	Yes	Yes	N/A
	Operate as Heat Pipe?	TPLTS	TPLTS	TPLTS	N/A
	Thermal Resistance (K/W)	0.019	0.020	0.022	N/A
	Comments	Liquid drains down walls in window 3, thin stream of liquid flows down walls in window 2.			N/A

(*continued on next page*)

Table 1 (*continued*)

Fill ratio		200 W	250 W	300 W	325 W
45%	Single- or Two-phase?	Two-phase	Two-phase	Two-phase	Maximum allowable temperature reached.
	Pulsation?	No	No	No	N/A
	Vapor After Condenser?	Yes	Yes	Yes	N/A
	Operate as Heat Pipe?	TPLTS	TPLTS	TPLTS	N/A
	Thermal Resistance (K/W)	0.024	0.025	0.025	N/A
	Comments	Liquid drains down walls in window 3, thin stream of liquid flows down walls in window 2.			N/A
40%	Single- or Two-phase?	Two-phase	Two-phase	Two-phase	Maximum allowable temperature reached.
	Pulsation?	No	No	No	N/A
	Vapor After Condenser?	Yes	Yes	Yes	N/A
	Operate as Heat Pipe?	TPLTS	TPLTS	TPLTS	N/A
	Thermal Resistance (K/W)	0.017	0.018	0.021	N/A
	Comments	Liquid drains down walls in window 3, thin stream of liquid flows down walls in window 2.			N/A
35%	Single- or Two-phase?	Two-phase	Two-phase	Two-phase	Maximum allowable temperature reached.
	Pulsation?	No	No	No	N/A
	Vapor After Condenser?	Yes	Yes	Yes	N/A
	Operate as Heat Pipe?	TPLTS	TPLTS	TPLTS	N/A
	Thermal Resistance (K/W)	0.019	0.020	0.021	N/A
	Comments	Initially liquid-vapor interface is visible in window 1. As temperature increases, vapor bubbles are generated and carry liquid up through window 1Liquid drains down walls in window 3 and window 2			
30%	Single- or Two-phase?	Two-phase	Two-phase	Maximum allowable temperature reached.	Maximum allowable temperature reached.
	Pulsation?	No	No	N/A	N/A
	Vapor After Condenser?	Yes	Yes	N/A	N/A
	Operate as Heat Pipe?	TPLTS	TPLTS	N/A	N/A
	Thermal Resistance (K/W)	0.020	0.021	N/A	N/A
	Comments	No liquid in window 1Liquid drains down walls in window 3 and window 2			
25%	Comments	Maximum allowable temperature reached.			

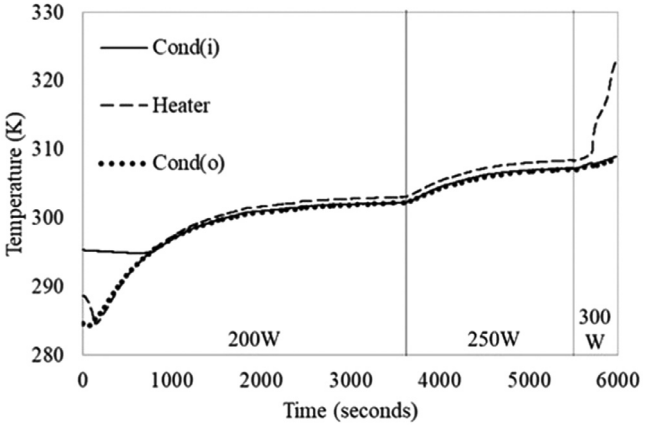

Fig. 5. Experimental temperature response to heat inputs of 200–300 W for a loop thermosyphon with fill ratio of 30% R134a.

liquid. However, due to the large spike in pressure when this condition is achieved, the experiment is not able to operate at the fully filled condition. The 95% experiment operates as a two-phase loop thermosyphon (TPLTS) until reaching the fully filled condition. However, the 90–30% fill ratio experiments operate as a TPLTS throughout the experiment until the maximum heat input is reached.

Fig. 6a shows the thermal resistance with varying fill ratio and heat input for the experiments discussed above, with error bars associated with the error propagation discussed previously. Thermal resistance for each fill ratio and heat input are summarized in Table 1. It can be seen from Fig. 6a that the thermal resistance increases with increasing heat input, indicating lower heat input experiments operate more effectively with R134a as the working fluid. There is no clear trend in thermal resistance with varying fill ratio. This may be because the range of heat inputs tested was not adequate to show trends with changing fill ratio. Fig. 6b shows the experimental temperature drop, the difference between the average evaporator and average condenser temperatures, for varying fill ratios and heat inputs. Temperature drop is highest for higher heat inputs, but there is no clear trend with respect to fill ratio.

The lowest thermal resistance and temperature drop occurs for the 80% and 75% fill ratios, followed closely by 40%, indicating a fill ratio between 75–80% or 40% R134a is ideal for the current experimental set-up.

Pictures and videos are taken throughout experiments at each of the flow visualization windows to observe flow trends. Fig. 7 shows pictures taken during the 95% fill ratio experiment. Initially, vapor bubbles are generated just after the heating element, as shown in Fig. 7a from window 1. The bubbles then rise to window 2, where they are slightly larger, more uniform, and more spread out (Fig. 7b) than in window 1. As time passes, the rate at which the vapor bubbles are generated and flow through windows 1 and 2 increases, and the size of the vapor bubbles decreases. As shown in Fig. 7c the bubbles in window 1 are smaller than in the beginning of the experiment (Fig. 7a). The same trend can be noted in Fig. 7d where the bubbles are smaller and closer together than they are in Fig. 7b for the flow through window 2.

As the 95% fill ratio experiment approaches the fully filled condition, the vapor bubbles grow continually smaller and rise faster until there is no longer any vapor in the system. No pictures of the flow through window 3 are shown since the flow remains a liquid at this location throughout the experiment.

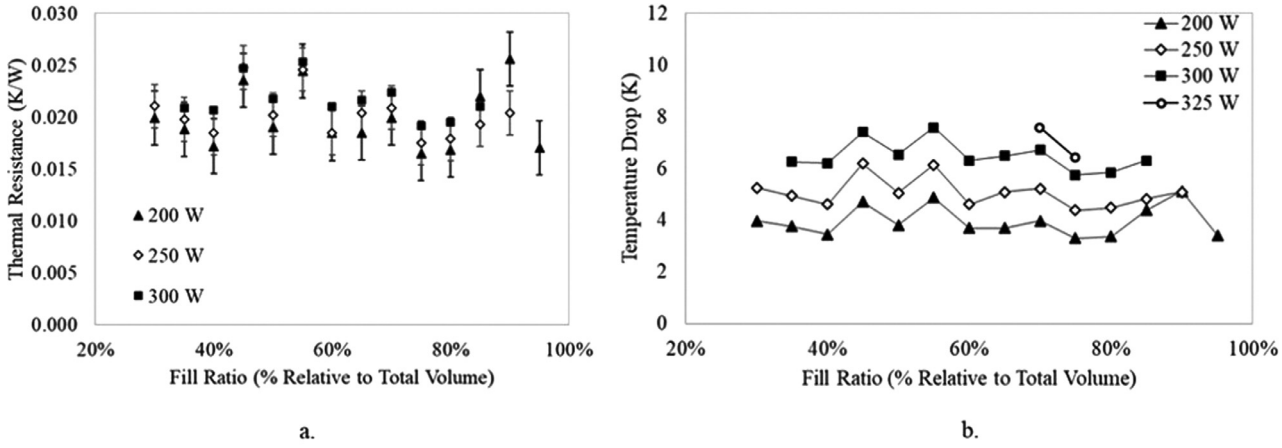

Fig. 6. Experimental a. thermal resistance and b. temperature drop with varying fill ratio and heat input with R134a as working fluid for a loop thermosyphon.

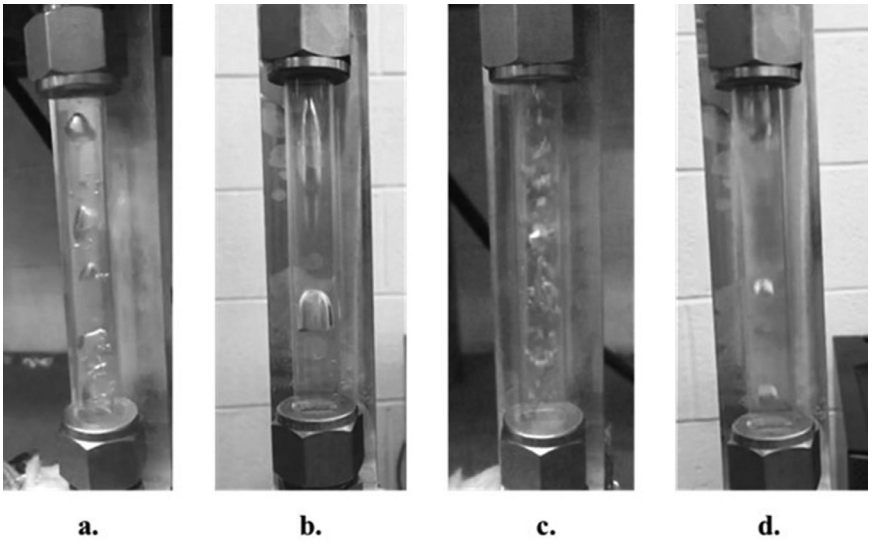

Fig. 7. Flow visualization for loop thermosyphon with fill ratio of 95% R134a and 200 W heat input at a. Window 1 at startup, b. Window 2 at startup, c. Window 1 at steady state, d. Window 2 at steady state.

When the fill ratio is decreased to 90%, slightly different trends are observed. Initially, as shown in Fig. 8a, small bubbles are generated from the evaporator section. These bubbles rise and merge to form large bubbles in window 2, as shown in Fig. 8b. As time progresses, the speed at which the bubbles are generated and flow through windows 1 and 2 increases. The size of the bubbles passing through window 2 increases. Fig. 8c shows the beginning of a large vapor bubble flowing through window 2, and Fig. 8d shows the tail end of the same bubble where the flow is disturbed by the high velocity of the vapor. There is also a pulsation phenomenon present in the 80–90% fill ratio experiments. There are several seconds where no vapor is present in either window 1 or 2, then a set of bubbles will flow through the windows, followed by another time segment of no bubbles. Presence of pulsation phenomenon for varying fill ratio and heat input are summarized in Table 1. No pictures of the flow through window 3 are shown since the working fluid remains a liquid at this location for the 90% fill ratio experiment.

Similar trends are observed for the 85–30% fill ratio experiments as in the 90% fill ratio experiment. However, in the experiments with fill ratios of 85% or less, vapor is present in window 3. Presence of vapor in window 3 (just after the condenser) is summarized in Table 1 for the varying fill ratios and heat inputs. As the temperature of the system increases and fill ratio decreases, more vapor appears in window 3. Fig. 9a shows window 3 for the 85% fill ratio experiment contains less vapor bubbles than the 80% fill ratio experiment, shown in Fig. 9b. There is also oscillation phenomenon noticed at window 3. The vapor travels downward, then flows back up towards the top of the loop, then there are several seconds where there is no vapor present in window 3 and the process repeats. This occurs for the 85–70% fill ratio experiments.

Another noticeable difference in fill ratio trends is in the 65% fill ratio experiment. In window 3, after 300 W of heat is applied, there are no vapor bubbles, but instead the interface between liquid in the lower portion of the experiment and vapor in the upper portion of the experiment is oscillating in this region, as seen in Fig. 9c.

When fill ratio decreases below 60%, the liquid-vapor interface is no longer visible in window 3. Instead, liquid drains down the walls after the condenser. As heat input increases, the speed of the liquid draining down the wall increases. For fill ratios less than 55%, the only liquid present in window 2 is a thin stream draining down the walls. For fill ratios of 30% or less, there is no liquid present in window 1. A thin stream of liquid is present in window 2, and a thicker stream of liquid is present in window 3. When 300 W of heat is applied to the 30% fill ratio experiment, the thin

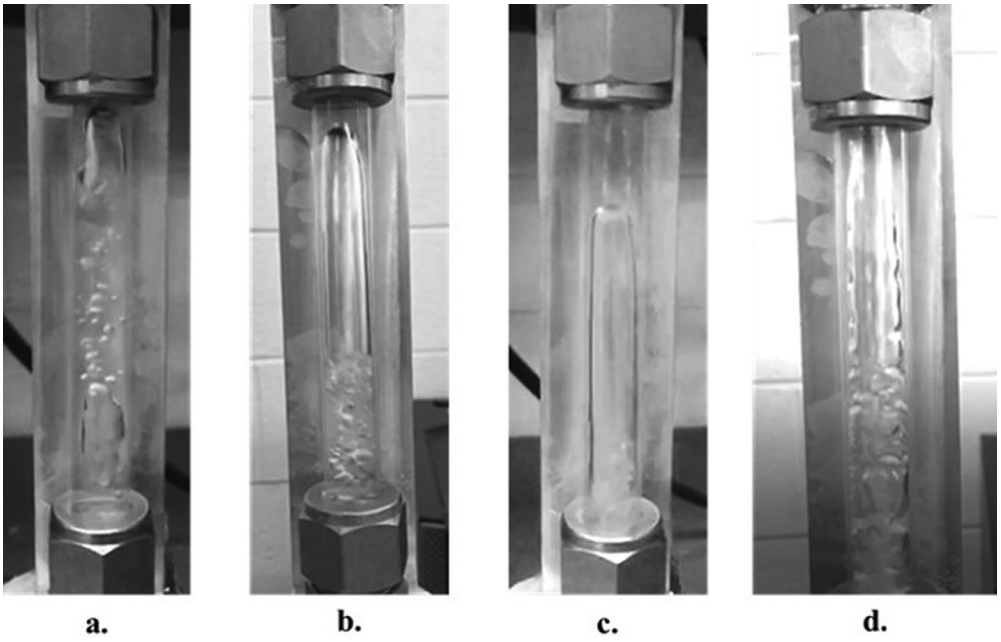

Fig. 8. Flow visualization for loop thermosyphon with fill ratio of 90% R134a at a. Window 1 at startup for 200 W heat input, b. Window 2 at startup for 200 W heat input, c. Window 1 at steady state for 250 W heat input, d. Window 2 at steady state for 250 W heat input.

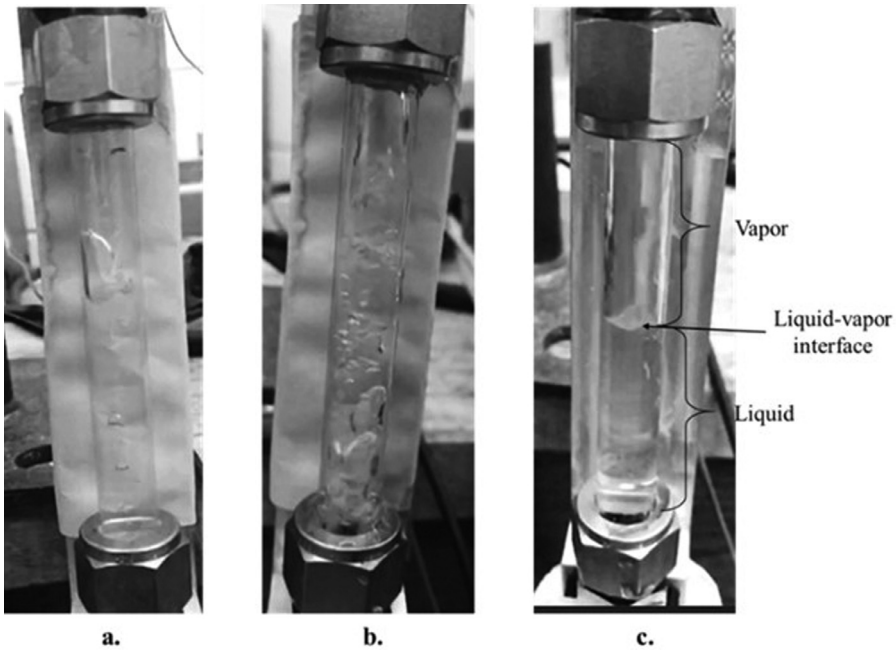

Fig. 9. Flow visualization of window 3 in loop thermosyphon with a. 85%, b. 80%, c. 65% fill ratios R134a.

stream of liquid in window 2 disappears. This corresponds to the point when the temperature after the heating element begins to increase rapidly and the working fluid is no longer able to circulate through the loop.

3.2. Effect of changing fill ratio with water as the working fluid

Before conducting experiments with water as the working fluid, all R134a is removed and the thermosyphon is cleaned. Using a funnel, distilled water is slowly poured into the top of the loop until no more air remains. The system is then sealed and rotated, while observing the flow visualization windows to ensure no air bubbles are present. The experiment is first run with a 100% water fill ratio. Temperature readings at the BC, just before the condenser inlet, TC, and just after the condenser outlet are shown in Fig. 10a. Results, including major trends and thermal resistance, are summarized in Table 2.

When the system is completely filled with water, it is able to reach steady state for heat inputs up to 350 W, which is the maximum heat input the heating element can run at. As shown in Fig. 10b, the thermal resistance of the 100% liquid water fill ratio experiment decreases linearly with increasing heat input. This indicates the system operates more efficiently for higher heat inputs with water as the working fluid.

Following the 100% liquid water fill ratio experiment, additional experiments are conducted where 10% of the original amount of

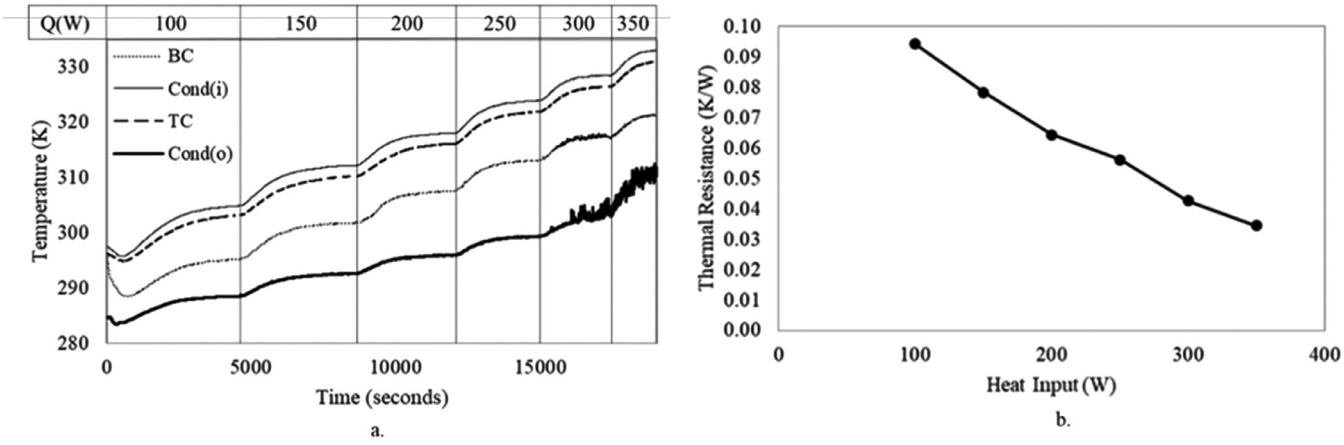

Fig. 10. Experimental a. Temperature response and b. Thermal resistance for a loop thermosyphon with 100% water fill ratio and heat inputs of 100–350 W.

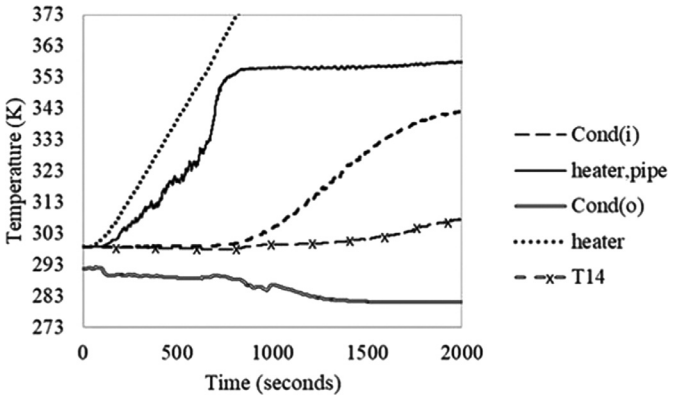

Fig. 11. Experimental temperature response for a loop thermosyphon with 90% water fill ratio and 100 W heat input.

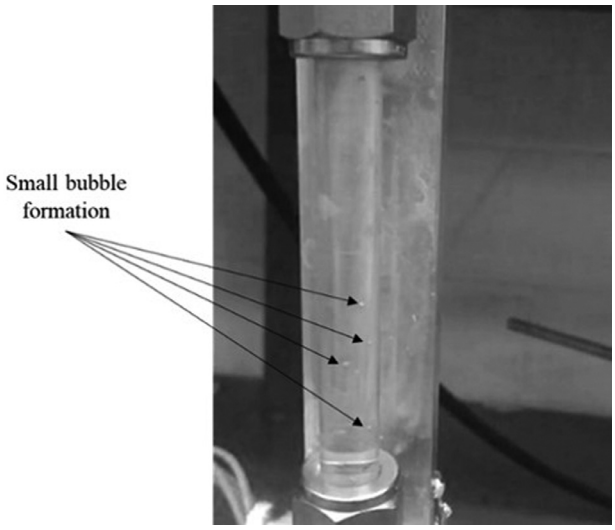

Fig. 12. Small bubble formation just after heating element for a loop thermosyphon with 90% water fill ratio with 100 W heat input.

water is removed each time, without allowing any air into the system. The lowest fill ratio tested is 30% of the total loop volume. An initial heat input of 100 W is applied to each experiment, increasing heat input by 50 W after each subsequent heat input reaches steady state. The temperature response for the first 2000 s for a 90% fill ratio in response to a 100 W heat input is shown in Fig. 11. Only the first 2000 s are shown to clearly illustrate the trends observed during the startup period. Thermocouple locations can be seen in Fig. 2.

There are several interesting trends to note in Fig. 11. First, the temperature of the pipe just after the heater increases with increasing temperature of the heating element until approximately 353 K (80 °C) is reached after which the temperature approaches a steady value. This is the point when small bubbles begin to appear in the flow visualization window just after the heating element, as shown in Fig. 12. It can be assumed that as soon as bubbles begin to form, latent heat is removed in order to form the bubbles, and the temperature of the water at the evaporator stops increasing, even though the heating element temperature continues to increase.

The point at which the temperature just after the heating element reaches a near constant value is the same time at which other temperatures farther from the evaporator begin to respond to the heat input. The temperature just before the condenser inlet begins to increase slowly, and the temperature just after the condenser outlet begins to decrease slowly. It can be seen in Fig. 11 that these changes in temperature begin after approximately 900 s, which indicates water starts flowing around the loop at this time.

A similar phenomenon is seen in the lower fill ratio experiments. The temperature responses for each fill ratio ranging from 90–30% of the total loop volume, in 10% increments, are shown in Fig. 13. Only the first 2000 s of data are shown for each experiment to clearly show the startup periods. An initial heat input of 100 W is applied to each experiment. As seen in Fig. 13, the same general trends can be seen in all fill ratio experiments from 90–30% water as discussed for the 90% fill ratio experiment shown in Fig. 11. First, the temperature just after the evaporator increases with the heating element temperature until a certain point where it begins to approach a steady value. At this point, small bubbles are seen in window 1, like those shown in Fig. 12. Shortly after the temperature of the pipe just after the heating element begins to level off, the working fluid begins to circulate through the loop and the temperatures around the entire system begin to respond: T14 and Cond(i) begin to increase and Cond(o) temperature begins to decrease slightly.

While the same general trends can be observed, there are several differences as fill ratio decreases. First, as seen in Fig. 13, the temperature at which the location just after the heating element approaches a constant value decreases with decreasing fill ratio. As water is removed from the system, the pressure inside the system

Table 2
Effects of water fill ratio on experimental performance of a loop thermosyphon.

Fill ratio		100 W	150 W	200 W	250 W	300 W	350 W
100%	Single- or Two-phase?	Single-phase	Single-phase	Single-phase	Single-phase	Single-phase	Single-phase
	Pulsation?	No	No	No	No	No	No
	Vapor After Condenser?	No	No	No	No	No	No
	Operate as Heat Pipe?	SPLTS	SPLTS	SPLTS	SPLTS	SPLTS	SPLTS
	Thermal Resistance (K/W)	0.094	0.078	0.064	0.056	0.043	0.034
	Comments	Large fluctuations began to appear in the temperature readings just after the condenser outlet for heat inputs greater than 250 W.					
90%	Single- or Two-phase?	Two-phase	Two-phase	Two-phase	Two-phase	Two-phase	Two-phase
	Pulsation?	No	No	Yes	Yes	Yes	Yes
	Vapor After Condenser?	No	No	No	No	No	No
	Operate as Heat Pipe?	TPLTS	TPLTS	TPLTS	TPLTS	TPLTS	TPLTS
	Thermal Resistance (K/W)	0.355	0.208	0.121	0.090	0.0766	0.0681
	Comments	N/A	N/A	N/A	N/A	N/A	N/A
80%	Single- or Two-phase?	Two-phase	Two-phase	Two-phase	Two-phase	Two-phase	Two-phase
	Pulsation?	No	No	Yes	Yes	Yes	Yes
	Vapor After Condenser?	No	No	No	No	No	No
	Operate as Heat Pipe?	TPLTS	TPLTS	TPLTS	TPLTS	TPLTS	TPLTS
	Thermal Resistance (K/W)	0.266	0.165	0.115	0.081	0.068	0.059
	Comments	N/A	N/A	N/A	For heat inputs of 250 W and greater, the water level can be seen fluctuating in the window at the top right of the loop.		
70%	Single- or Two-phase?	Two-phase	Two-phase	Two-phase	Two-phase	Two-phase	Two-phase
	Pulsation?	No	No	Yes	Yes	Yes	Yes
	Vapor After Condenser?	No	No	No	No	No	No
	Operate as Heat Pipe?	TPLTS	TPLTS	TPLTS	TPLTS	TPLTS	TPLTS
	Thermal Resistance (K/W)	0.270	0.153	0.105	0.078	0.055	0.057
	Comments	N/A	N/A	For heat inputs of 200 W and greater, the water level can be seen fluctuating in the window at the top right of the loop.			
60%	Single- or Two-phase?	Two-phase	Two-phase	Two-phase	Two-phase	Two-phase	Two-phase
	Pulsation?	No	No	Yes	Yes	Yes	Yes
	Vapor After Condenser?	No	No	Yes	Yes	Yes	Yes
	Operate as Heat Pipe?	TPLTS	TPLTS	TPLTS	TPLTS	TPLTS	TPLTS
	Thermal Resistance (K/W)	0.235	0.111	0.072	0.073	0.0064	0.090
	Comments	N/A	For heat inputs of 150 W and greater, the water level can be seen fluctuating in the window at the top right of the loop.				
		N/A	N/A	N/A	Water level can be seen fluctuating in window after condenser for heat inputs of 250 W or greater.		
50%	Single- or Two-phase?	Two-phase	Two-phase	Two-phase	Two-phase	Two-phase	Two-phase
	Pulsation?	Yes	Yes	Yes	Yes	Yes	Yes
	Vapor After Condenser?	Yes	Yes	Yes	Yes	Yes	Yes
	Operate as Heat Pipe?	TPLTS	TPLTS	TPLTS	TPLTS	TPLTS	TPLTS
	Thermal Resistance (K/W)	0.177	0.139	0.121	0.112	0.110	0.097
	Comments	Water level can be seen fluctuating in the flow visualization window at the top right section of the loop and just after the condenser for all heat inputs greater than 100 W.					
40%	Single- or Two-phase?	Two-phase	Two-phase	Two-phase	Two-phase	Two-phase	Two-phase
	Pulsation?	Yes	Yes	Yes	Yes	Yes	Yes
	Vapor After Condenser?	Yes	Yes	Yes	Yes	Yes	Yes
	Operate as Heat Pipe?	TPLTS	TPLTS	TPLTS	TPLTS	TPLTS	TPLTS
	Thermal Resistance (K/W)	0.165	0.093	0.074	0.068	0.071	0.071
	Comments	Water drains down the walls of the flow visualization window just after the condenser for all heat inputs greater than 100 W.					
30%	Single- or Two-phase?	Two-phase	Two-phase	Two-phase	Two-phase	Two-phase	Two-phase
	Pulsation?	No	No	No	No	No	No
	Vapor After Condenser?	Yes	Yes	Yes	Yes	Yes	Yes
	Operate as Heat Pipe?	TPLTS	TPLTS	TPLTS	TPLTS	TPLTS	TPLTS
	Thermal Resistance (K/W)	0.411	0.299	0.231	0.187	0.157	0.135
	Comments	Very small trickles of liquid drained down the walls of the flow visualization window just after the condenser for all heat inputs.					

decreases to below atmospheric pressure and continues decreasing as more water is removed, resulting in a lower boiling temperature. Therefore, the temperature at which bubbles begin to form also decreases with decreasing fill ratio.

The time it takes for working fluid to begin circulating and for temperatures farther away from the heating element (T14, Cond(i), Cond(o)) to begin responding to the heat input increases with decreasing fill ratio. The times at which this occurs for the 90%, 80%, 70%, 60%, 50%, 40%, and 30% (not seen on figure) fill ratios are approximately 900, 1200, 1400, 1600, 1800, 1900, and 2900 s, respectively. The 30% fill ratio experiment takes much longer to reach the point where heat is transferred, indicating the fill ratio is too low for heat to be transferred effectively.

The thermal resistance for each fill ratio and heat input is plotted in Fig. 14a. As seen in Fig. 14a, there is not a large difference in thermal resistance for the 100% fill ratio experiment for different heat inputs, although it can clearly be seen that the thermal resistance decreases with increasing heat input. The thermal resistance generally decreases with increasing heat input for each fill ratio experiment, except the 60% and 40% experiments. The difference in thermal resistance for the 200–300 W experiments with fill ratios of 40% and 60% are very small, indicating that within this range for these fill ratios, thermal resistance is independent of heat input. The differences in the 40% fill ratio experiments are within the error associated with each value. Fig. 14b shows the thermal resistance for three fill ratios, with respect to heat input. It can be

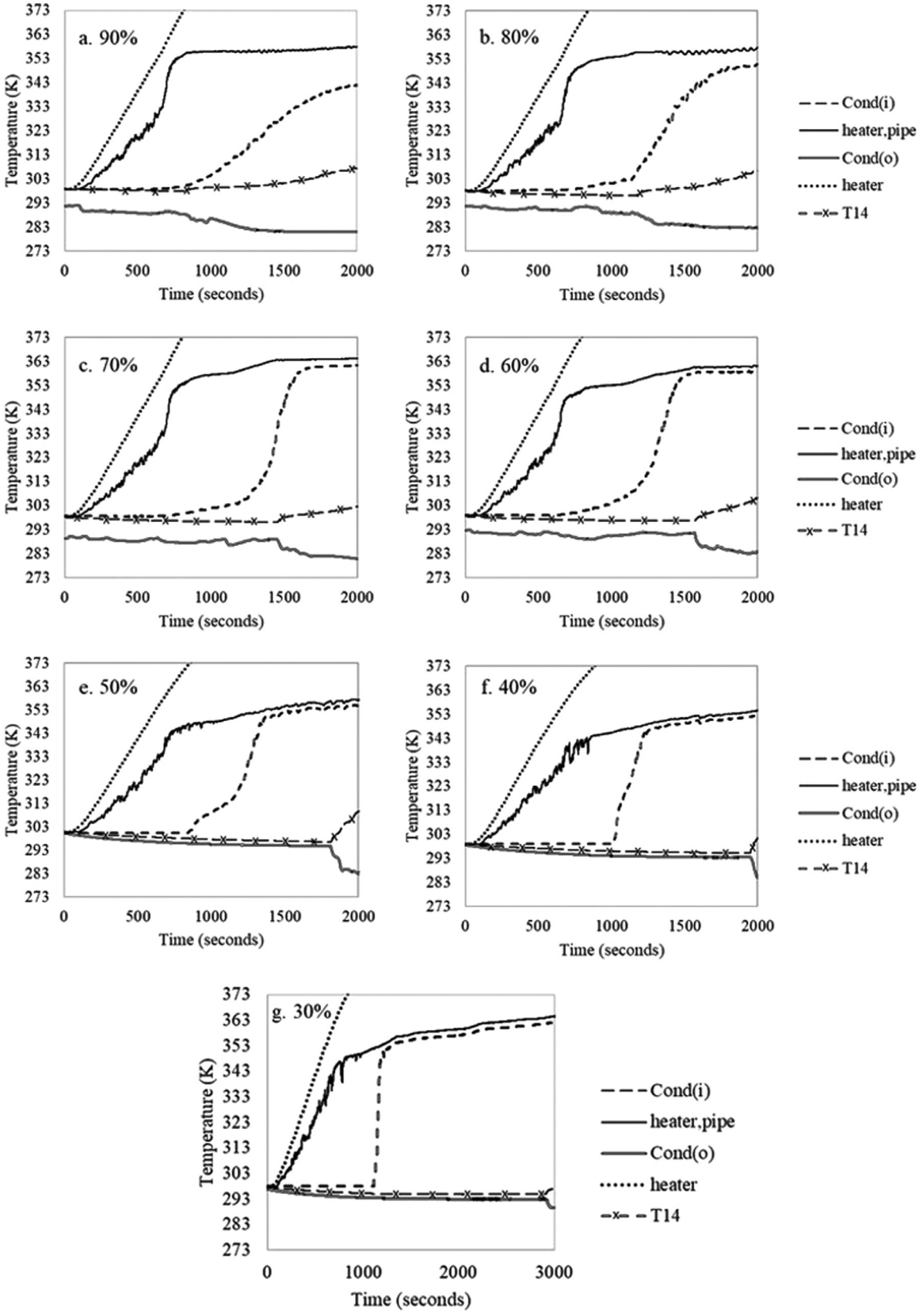

Fig. 13. Temperature response to a heat input of 100 W for a loop thermosyphon with water fill ratios of a. 90% b. 80% c. 70% d. 60% e. 50% f. 40% and g. 30%.

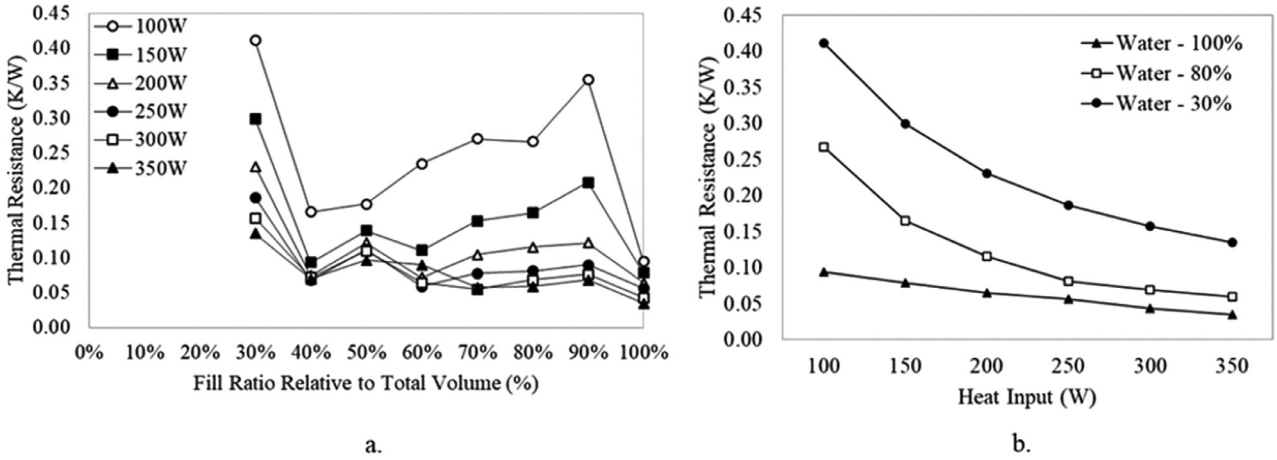

Fig. 14. Effects of a. Fill ratios of 100–30% water and b. Heat inputs of 100–350 W on experimental thermal resistance for a loop thermosyphon.

seen in Fig. 14b the thermal resistance decreases with heat input for each fill ratio shown. However, the decrease in thermal resistance is linear for a fill ratio of 100%, but for fill ratios of 30% and 80%, the slope of the decreasing thermal resistance decreases with increasing heat input. This indicates the step change in thermal resistance is more uniform for the 100% fill ratio when the experiment operates as a SPLTS than for lower fill ratios operating as a TPLTS.

For each heat input, the lowest thermal resistance occurs for the 100% fill ratio. For the 100 W heat input, the thermal resistance is at a minimum for the 100% fill ratio experiment then increases substantially for the 90% fill ratio experiment. Then, as fill ratio decreases below 90%, there is a general decreasing trend in thermal resistance. For the heat inputs greater than 100 W, this trend is less clear. When the fill ratio is decreased to 30%, the thermal resistance is at a maximum for each heat input. The 30% fill ratio experiment is the least effective. The most effective fill ratios for this experiment are either the 100% fill ratio where the system operates as a single-phase loop thermosyphon (SPLTS) or the 40% fill ratio experiment where the system operates as a two-phase loop thermosyphon (TPLTS).

Flow visualization is discussed below for the 90% fill ratio experiment. After heat is applied, there remains liquid in all three flow visualization windows. Once the water temperature at the heating element reaches the boiling temperature at the system pressure, small bubbles begin to form just after the evaporator window as shown in Fig. 12.

As time progresses and temperature around the loop increases, the size and speed of bubbles flowing through the flow visualization window just after the evaporator increases. Fig. 15 shows the flow visualization windows just after evaporator (a) and at the top right of the loop (b) at the steady state operation of the 90% fill ratio experiment with a heat input of 100 W.

As heat input and therefore temperature of the system increases, the size and speed of the vapor bubbles increase. Fig. 15c and 15d show the flow through the system at steady state for a heat input of 350 W for the 90% fill ratio experiment. When comparing Fig. 15a and 15b with Fig. 15c and 15d, the bubble size is larger for the higher heat input.

The startup for the 80% fill ratio experiment is similar to that of the 90% fill ratio experiment. After the temperature of the working fluid at the heating element reaches the boiling temperature at the system pressure, small bubbles begin to form and flow through the flow visualization window just after the evaporator, similar to those in Fig. 12. As the system reaches steady state for the 100 W heat input, the size and speed of the vapor bubbles just after the condenser increase. Initially, the water level is such that it can be seen in the flow visualization window on the top right of the loop, as seen in Fig. 16a. As the system temperature increases after a 100 W heat input is applied, the water level rises to be above this window and only small bubbles are seen rising through the flow visualization window at the top right of the loop as seen in Fig. 16b. As the heat input is increased to 200 W, the speed of the small vapor bubbles rising through the flow visualization window at the top right of the loop increases. As heat input is increased and the temperature within the system increases, the size and speed of the vapor bubbles just after the evaporator increases. There is also a pulsation phenomenon that occurs for heat inputs of 200 W and higher where there are several seconds of only liquid just after the evaporator followed by several seconds of vapor shooting upwards.

For heat inputs of 250 W and higher, the water level can again be seen in the window at the top right of the loop. However, there is now a large fluctuation in the location of the water level. Fig. 16c shows the flow visualization window at the top right of the loop for a heat input of 350 W. As seen in Fig. 16, the water level fluctuates. In Fig. 16c, there is entirely liquid in this section. Then, bubbles start to appear in Fig. 16d rising from the evaporator. After several seconds, the water level drops and can be seen near the bottom of the window in Fig. 16e. Then, the water level rises again as seen in Fig. 16f until it is eventually above the window and there is only liquid present in this section, and the process repeats. As heat input increases, the speed at which this process occurs increases.

When the experiment is 70% filled with liquid water, the water level is initially below the level of window 2 and cannot be seen. When 100 W of heat is applied to the heating element, vapor is generated at the heating element in a similar process as the 80% fill ratio experiment. Eventually, enough vapor is generated at the evaporator that the vapor rises, and the liquid level rises above window 2 and only small bubbles are seen flowing through an otherwise entirely liquid section, similar to the low heat inputs of the 80% fill ratio experiment shown in Fig. 16. The flow through window 3 remains entirely liquid throughout the experiment. The same flow trends are seen for the 150 W heat input as the 100 W heat input. As the heat input is increased to 200 W, the water level can again be seen in the flow visualization window at the top right of the loop and the process described in Fig. 16 can be observed.

For heat inputs of 250–350 W, the water level is sometimes below window 2. Fig. 17 shows the flow visualization window at four separate times during the 70% fill ratio experiment with a heat input of 350 W. In Fig. 17a, the water level can be seen in window 2.

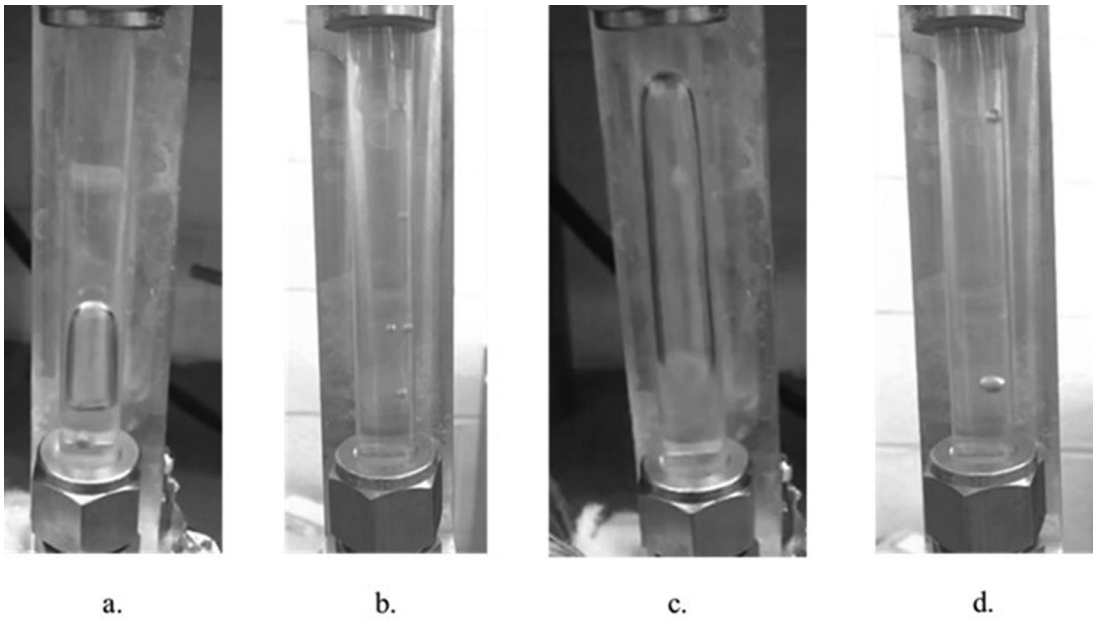

Fig. 15. Flow visualization for a loop therosyphon with a 90% water fill ratio at a. Window 1 with heat input of 100 W, b. Window 2 with a heat input of 100 W, c. Window 1 with heat input of 350 W, d. Window 2 with heat input of 350 W.

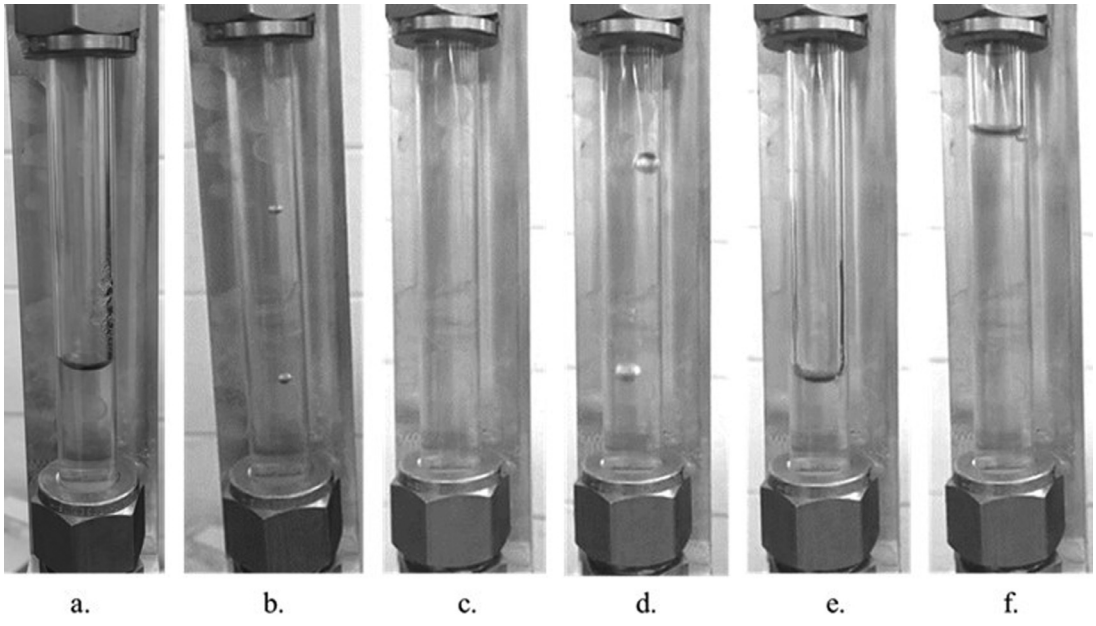

Fig. 16. Flow visualization of a loop thermosyphon at window 2 for a fill ratio of 80% water a. Before heat is applied and b. at steady state for a 100 W heat input c., d., e., f., During 350 W heat input.

Then, the water level rises and window 2 is filled entirely with liquid as shown in Fig. 17b. Next, vapor bubbles begin to flow through the window as seen in Fig. 17c. After several seconds, the water level drops below window 2 and liquid flows down the sides of the walls as shown in Fig. 17d until the water level rises again and the process repeats. These observations also occur for heat inputs of 300 W and 350 W. However, the speed of fluctuations increases as heat input increases.

During the startup period of the 60% fill ratio experiment after 100 W of heat is applied to the evaporator, the flow through window 1 is similar to the flow for the 70% and 80% fill ratio experiments. The flow through window 2 for the 100 W heat input is similar to that shown in Fig. 16 where the liquid line appears in the window and then moves back up. The liquid line does not drop below window 2 until the heat input is increased to 150 W, when the flow behaves as the flow shown in Fig. 17 where the liquid line fluctuates above and below window 2. This trend also occurs for all heat inputs greater than 150 W. The speed of the fluctuation increases with heat input.

The pulsation phenomenon discussed previously can clearly be seen in the 60% fill ratio experiment when a heat input of 200 W is applied. Fig. 18 shows the flow visualization window just after the evaporator. In the beginning of the cycle, window 1 is filled entirely with liquid, as shown in Fig. 18a. Then, small vapor bubbles start to appear and continue to increase in size as seen in Fig. 18b and 18c. After several seconds of the smaller bubbles, large vapor bubbles begin to appear in window 1, as shown in Fig. 18d. Several seconds later, all vapor bubbles in this section disappear

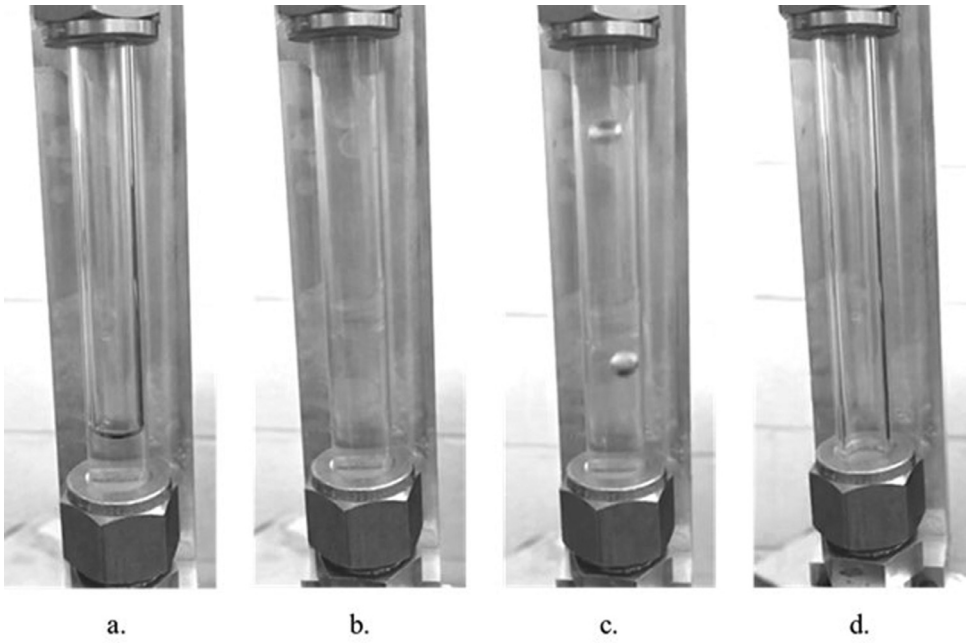

Fig. 17. Flow visualization at window 2 for 70% water fill ratio loop thermosyphon and 250 W heat input as time progresses from a. to d.

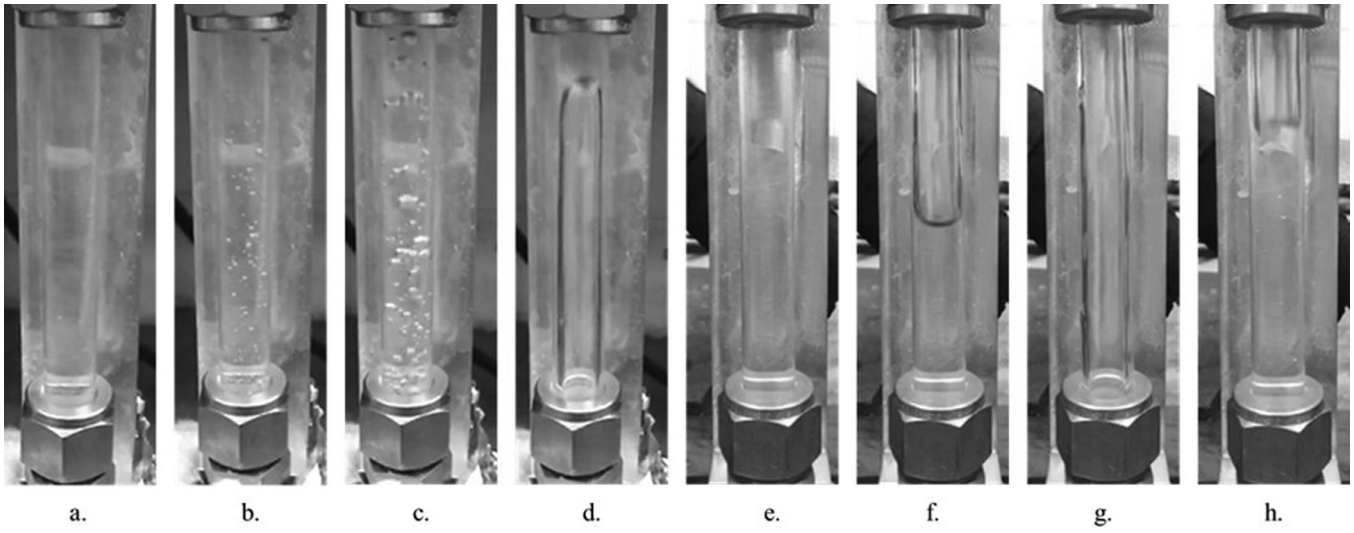

Fig. 18. Flow visualization for 60% water fill ratio loop thermosyphon at a.-d. Window 1 with 200 W heat input e.-h. Window 3 with 250 W heat input.

and window 1 is again entirely liquid and the process repeats. As heat input is increased from 200 W to 250 W, the pulsation becomes more pronounced and the time that each segment lasts (liquid only, small vapor bubbles, then large bubbles) increases.

For fill ratios greater than 60%, the working fluid flowing through window 3 remains liquid throughout the experiment. However, for heat inputs of 250 W or greater for 60% fill ratio, vapor can be seen in this section. Fig. 18e.–h. shows the flow visualization window just after the condenser for the 250 W heat input to the 60% fill ratio experiment. Initially there is entirely liquid in this section, as seen in Fig. 18e. Then, the water level drops in Fig. 18f and drops below window 3 in Fig. 18g. Shortly thereafter, a stream of liquid flows down the walls and the liquid level again rises as seen in Fig. 18h until it is above the window and the process repeats.

Flow trends for the 50% fill ratio experiment are similar to those of the 60% fill ratio experiment. Presence of pulsation and vapor in window 3 is summarized in Table 2.

Flow trends for the 40% fill ratio experiment are similar to those of the 60% fill ratio experiment at windows 1 and 2. Presence of pulsation in the flow and vapor in window 3 are summarized in Table 2. The liquid level is no longer visible in window 3. Instead, liquid can be seen draining down the walls of this section. For the 100 W heat input, there is only a small trickle of water draining down the walls of window 3. As the heat input increases, the thickness and speed of the film flowing down the walls increases.

The flow through window 1 for the 30% fill ratio experiment is similar to the fill ratios mentioned previously. Presence of pulsation is summarized in Table 2. For a heat input of 100 W, there is no liquid present in windows 2 or 3. For heat inputs of 150 W and greater, a large vapor bubble flows very fast up through window 2. Ahead of the bubble there is a small section of liquid which then drains down the walls of window 2 after the bubble passes through. This continues to occur, with one large bubble rising at a time. As heat input increases, the speed at which the large vapor bubble rises increases. The beginning of one large vapor bubble is

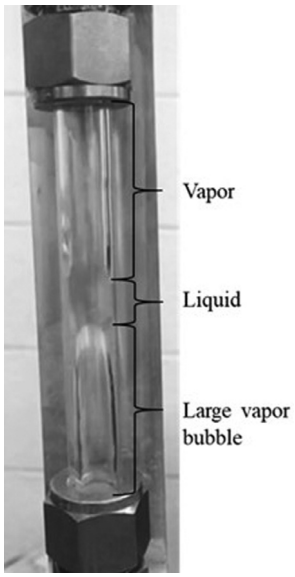

Fig. 19. Flow visualization at window 2 for 30% water fill ratio loop thermosyphon and 150 W heat input.

shown in Fig. 19 pushing a small amount of liquid up. This liquid then drains down the walls.

As heat input increases above 100 W, a small trickle of liquid begins to drain down the walls of window 3.

3.3. Comparison of effects of changing fill ratio between working fluids

For the vertical orientation with the evaporator below the condenser, thermal resistance is compared between R134a and water as working fluids for fill ratios of 100–30% of the total volume and heat inputs of 200–350 W. Results are shown in Table 3. The experiments with R134a as working fluid are not able to reach steady state for heat inputs of 350 W due to maximum allowable temperature of 323 K being reached. This is denoted in Table 2. The experimental thermal resistance for all fill ratios and heat inputs where the experiment is able to reach steady state with working fluid of water or R134a are listed in Table 3. The thermal resistance is higher for the experiments with water as the working fluid. The final column calculates how many times larger the thermal resistance is for water as the working fluid than R134a. This multiple ranges from 2.7–12.2 depending on fill ratio and heat input. These results indicate the experiment operates more effectively with R134a as the working fluid for all conditions where the experiment can reach steady state. However, with water as the working fluid, the experiment can operate at a fill ratio up to 100% and heat inputs up to 350 W. Therefore, if the objective is to run the thermosyphon with a fill ratio of 100% or if the heat that needs to be transferred is between 300–350 W, water should be chosen as the working fluid.

An important trend to note for thermal resistance in response to increasing heat input between the two working fluids is: with R134a as the working fluid, thermal resistance increases with increasing heat input, but thermal resistance decreases with increasing heat input when water is the working fluid. This indicates the R134a loop thermosyphon operates more efficiently at lower heat inputs, and the water loop thermosyphon operates more efficiently at higher heat inputs.

Another noticeable difference between the water and R134a experiments is the startup period. The startup period for all fill ratios with R134a is similar to the startup of the 100% water experiment. In these experiments, all the temperatures around the loop respond quickly to the heat input and increase steeply before gradually reaching steady state. However, the experiments with water as the working fluid for fill ratios of 90% or less consist of a very different startup period, described previously. The differences in these startup periods is because the working fluid in the R134a experiments and the 100% water fill ratio experiment are initially at saturation conditions. However, for water with fill ratios of 90% or less, the system must reach saturated conditions before heat can be transferred around the loop.

The trends in flow visualization are similar for both working fluids. The fill ratios and heat inputs at which pulsation are present and where there is vapor in window 3 vary and can be seen in the respective tables. However, the speed and size of the vapor bubbles generated at the evaporator increase with increasing temperature for both working fluids, except when the R134a experiment approaches the fully filled condition and bubble size decreases. One notable difference is that the flow of liquid/vapor water is more uniform than that of R134a. These trends can be seen in the respective flow visualization pictures.

4. Effect of changing inclination angle

The effect of inclination was studied to determine if the loop thermosyphon is able to transfer heat against gravity and operate in the counter-gravity orientation.

4.1. Effect of changing inclination angle with R134a as the working fluid

The experiment is run at four different inclination angles (vertical with evaporator below condenser, at a 45° angle with evaporator below condenser, horizontal, and vertical with evaporator above condenser) with three different fill ratios (90%, 75%, and 60% relative to the total volume) R134a. The results are summarized in Table 4 for the three different fill ratios. Of the four orientations, the thermosyphon operated as a TPLTS when oriented vertically (with evaporator below condenser) and at a 45° angle to the horizontal (with evaporator below condenser). It can be assumed that the thermosyphon is also able to operate as a TPLTS for angles greater than 45° to the horizontal where the evaporator is below the condenser. The thermosyphon is not able to transfer heat when horizontal (evaporator level with condenser) or with the evaporator above the condenser. The orientations at which the thermosyphon can or cannot operate are consistent for all three fill ratios tested. Therefore, the thermosyphon is not able to transfer heat against gravity for any of the fill ratios tested.

The thermal resistance for the vertical (with evaporator below condenser) is slightly lower than the 45° angle to the horizontal (with evaporator below condenser) experiment for corresponding heat inputs for the 90% fill ratio. This indicates the thermosyphon can operate slightly more effectively in the vertical orientation when the fill ratio is 90%.

When the fill ratio is 75%, the thermal resistance for the vertical orientation is slightly lower than the 45° angle experiment for corresponding heat inputs, similar to the 90% fill ratio experiments. This indicates the thermosyphon operates slightly more effectively in the vertical orientation. Vapor bubbles appear in the flow visualization window just after the condenser for the vertical experiment for all heat inputs, but not for the 45° angle orientation.

The 60% fill ratio experiment can reach steady state for heat inputs up to 350 W, whereas the 90% and 75% fill ratio experiments are only able to reach steady state for heat inputs of 300 W or less. For the 60% fill ratio experiment, the thermal resistance for the 45° inclination angle is less than the thermal resistance in the vertical orientation for the same heat inputs. This is opposite

Table 3
Thermal resistance for experiments with water and R134a as working fluids with fill ratios from 100–30% and heat inputs of 200–350 W for a loop thermosyphon.

		Thermal resistance (K/W)		
Fill ratio	Heat input (W)	Working fluid: R134a	Working fluid: water	R for water is higher than R134a by:
100%	200	max temp reached	0.064	N/A
	250	max temp reached	0.056	N/A
	300	max temp reached	0.043	N/A
	350	max temp reached	0.034	N/A
90%	200	0.026	0.121	4.7x
	250	0.020	0.090	4.5x
	300	max temp reached	0.077	N/A
	350	max temp reached	0.068	N/A
80%	200	0.017	0.115	6.8x
	250	0.018	0.081	4.5x
	300	0.019	0.068	3.6x
	350	max temp reached	0.059	N/A
70%	200	0.017	0.105	6.2x
	250	0.018	0.078	4.3x
	300	0.019	0.055	2.9x
	350	max temp reached	0.057	N/A
60%	200	0.018	0.072	4.0x
	250	0.020	0.059	3.0x
	300	0.022	0.064	2.9x
	350	max temp reached	0.090	N/A
50%	200	0.024	0.121	5.0x
	250	0.025	0.112	4.5x
	300	0.025	0.110	4.4x
	350	max temp reached	0.097	N/A
40%	200	0.024	0.074	3.1x
	250	0.025	0.068	2.7x
	300	0.025	0.071	2.8x
	350	max temp reached	0.070	N/A
30%	200	0.019	0.231	12.2x
	250	0.020	0.187	9.4x
	300	0.021	0.157	7.5x
	350	max temp reached	0.135	N/A

what is observed in the 90% and 75% fill ratio experiments. When the fill ratio is 60%, the thermosyphon operates slightly more efficiently when angled at 45° to the horizontal than vertically, with the evaporator below the condenser. Vapor bubbles appear in the flow visualization window just after the condenser for the vertical experiment for all heat inputs, but only for the 300 W and 350 W experiments at the 45° angle orientation.

The thermosyphon can operate as a TPLTS for all three R134a fill ratios tested when the thermosyphon is oriented with the evaporator below the condenser. When the evaporator is level with or above the condenser, the thermosyphon is not able to transfer heat. Therefore, the R134a loop thermosyphon requires the evaporator to be below the condenser in order to operate and relies on gravity for the flow of working fluid, as is expected.

4.2. Effect of changing inclination angle with water as the working fluid

The experiment was filled with 100%, 90%, and 75% (of the total loop volume) water and each fill ratio is tested at four inclination angles. The thermosyphon was tested vertically (with evaporator below condenser), at a 45° angle to the horizontal (with evaporator below condenser), horizontally, and vertically (with evaporator above condenser). The results are summarized in Table 5. Of these orientations, the thermosyphon operates as a SPLTS when tested vertically (with evaporator below condenser) and at a 45° angle to the horizontal (with evaporator below condenser) when the initial fill ratio is 100%, and as a two-phase loop thermosyphon (TPLTS) for these two orientations when the fill ratio is 90% and 75%. It can be assumed that the thermosyphon is also able to operate as a SPLTS or TPLTS, for the respective fill ratios, for angles greater than 45° to the horizontal where the evaporator is below the condenser. The thermosyphon is not able to transfer heat when horizontal (evaporator level with condenser) or with the evaporator above the condenser for any fill ratio tested. Therefore, the flow of working fluid relies on gravity for the 100%, 90%, or 75% fill ratios, as is expected.

Fig. 20 shows the graph of thermal resistance for the 75%, 90%, and 100% fill ratio experiments for the orientations at which the thermosyphon is able to operate. The thermal resistance for each heat input and orientation is listed in Table 5. Interestingly, the thermal resistance for the vertical orientation is greater than that of the 45° orientation for the first three heat inputs (100–200 W). When the heat input is greater than 200 W, the thermal resistance is slightly lower for the vertical orientation than the 45° orientation. This indicates the optimal orientation angle for the 100% fill ratio experiment depends on heat input. The thermosyphon operates more effectively in the vertical orientation for heat inputs of 250–350 W and operates more effectively in the 45° orientation for heat inputs of 100–200 W.

As seen in Fig. 20, the thermal resistance for the 90% fill ratio for both orientations are very similar with an average percent difference of 3.6% and a maximum percent difference of 7.5% for the 300 W heat input. A similar trend can be noted for the 100% fill ratio experiment, where the orientation with the lowest thermal resistance depends on heat input. For the 90% fill ratio experiment with a heat input of 100 W, the lower thermal resistance occurs for the 45° orientation, whereas for heat inputs of 150–350 W, the vertical orientation has lower thermal resistance than the 45° orientation.

A similar trend can be noted for the 75% fill ratio, where there is a cutoff heat input at which the optimal orientation switches.

Table 4
Effects of inclination angle on performance of R134a loop thermosyphon with fill ratios of 90%, 75%, 60%.

Fill ratio	Orientation		200 W	250 W	300 W	350 W
90%	Vertical (evaporator below condenser)	Single- or Two-phase?	Two-phase	Two-phase	Two-phase	Maximum allowable temperature reached.
		Pulsation?	Yes	Yes	No	N/A
		Vapor After Condenser?	No	No	No	N/A
		Operate as Heat Pipe?	TPLTS	TPLTS	TPLTS	N/A
		Thermal Resistance (K/W)	0.019	0.021	0.017	N/A
		Comments	Pulsation phenomenon occurred for the 200 W and 250 W experiments where there are a few seconds in the flow visualization windows just after the evaporator and near the top of the loop where vapor bubbles would appear, followed by several seconds of no bubbles.			N/A
	45° (evaporator below condenser)	Single- or Two-phase?	Two-phase	Two-phase	Maximum allowable temperature reached.	
		Pulsation?	No	No		
		Vapor After Condenser?	No	No		
		Operate as Heat Pipe?	TPLTS	TPLTS		
		Thermal Resistance (K/W)	0.021	0.022		
		Comments				
	Horizontal	Comments	Heat input is initially set to 100 W. The temperatures near the evaporator increased very quickly while the remainder of the temperatures around the loop remained relatively constant. The heat input needed to be shut off, so the experiment did not reach the maximum temperature. Steady State was not reached.			
	Vertical (evaporator above condenser)	Comments	Similar phenomenon is seen as in the horizontal orientation, except the temperature increase is steeper in the anti-gravity orientation.			
75%	Vertical (evaporator below condenser)	Single- or Two-phase?	Two-phase	Two-phase	Two-phase	Maximum allowable temperature reached.
		Pulsation?	Yes	Yes	Yes	N/A
		Vapor After Condenser?	Yes	Yes	Yes	N/A
		Operate as Heat Pipe?	TPLTS	TPLTS	TPLTS	N/A
		Thermal Resistance (K/W)	0.020	0.020	0.021	N/A
		Comments	Pulsation phenomenon occurred for the 200–300 W experiments where there are a few seconds in the flow visualization windows just after the evaporator and near the top of the loop where vapor bubbles would appear, followed by several seconds of no bubbles.			N/A
	45° (evaporator below condenser)	Single- or Two-phase?	Two-phase	Two-phase	Two-phase	Maximum allowable temperature reached.
		Pulsation?	Yes	Yes	Yes	N/A
		Vapor After Condenser?	No	No	No	N/A
		Operate as Heat Pipe?	TPLTS	TPLTS	TPLTS	N/A
		Thermal Resistance (K/W)	0.028	0.025	0.024	N/A
		Comments	N/A	N/A	N/A	N/A
	Horizontal	Comments	Heat input is initially set to 100 W. The temperatures near the evaporator increased very quickly while the remainder of the temperatures around the loop remained relatively constant. The heat input needed to be shut off, so the experiment did not reach the maximum temperature. Steady State was not reached.			
	Vertical (evaporator above condenser)	Comments	Similar phenomenon is seen as in the horizontal orientation, except the temperature increase is steeper in the anti-gravity orientation.			
60%	Vertical (evaporator below condenser)	Single- or Two-phase?	Two-phase	Two-phase	Two-phase	Two-phase
		Pulsation?	No	No	No	No
		Vapor After Condenser?	Yes	Yes	Yes	Yes
		Operate as Heat Pipe?	TPLTS	TPLTS	TPLTS	TPLTS
		Thermal Resistance (K/W)	0.023	0.022	0.022	0.021
		Comments				
	45° (evaporator below condenser)	Single- or Two-phase?	Two-phase	Two-phase	Two-phase	Two-phase
		Pulsation?	No	No	No	No
		Vapor After Condenser?	No	No	Yes	Yes
		Operate as Heat Pipe?	TPLTS	TPLTS	TPLTS	TPLTS
		Thermal Resistance (K/W)	0.018	0.018	0.018	0.018
		Comments				
	Horizontal	Comments	Heat input is initially set to 100 W. The temperatures near the evaporator increased very quickly while the remainder of the temperatures around the loop remained relatively constant. The heat input needed to be shut off, so the experiment did not reach the maximum temperature. Steady State was not reached.			
	Vertical (evaporator above condenser)	Comments	Similar phenomenon is seen as in the horizontal orientation, except the temperature increase is steeper in the anti-gravity orientation.			

Table 5
Effects of inclination angle on performance of water loop thermosyphon with fill ratios of 100%, 90%, and 75%.

Fill ratio	Orientation		100 W	150 W	200 W	250 W	300 W	350 W
100%	Vertical (evaporator below condenser)	Single- or Two-phase?	Single-phase	Single-phase	Single-phase	Single-phase	Single-phase	Single-phase
		Pulsation?	No	No	No	No	No	No
		Vapor After Condenser?	No	No	No	No	No	No
		Operate as Heat Pipe?	SPLTS	SPLTS	SPLTS	SPLTS	SPLTS	SPLTS
		Thermal Resistance (K/W)	0.094	0.078	0.064	0.056	0.043	0.034
		Comments	Working fluid remained single phase throughout experiment.					
	45° (evaporator below condenser)	Single- or Two-phase?	Single-phase	Single-phase	Single-phase	Single-phase	Single-phase	Maximum allowable temperature reached.
		Pulsation?	No	No	No	No	No	N/A
		Vapor After Condenser?	No	No	No	No	No	N/A
		Operate as Heat Pipe?	SPLTS	SPLTS	SPLTS	SPLTS	SPLTS	N/A
		Thermal Resistance (K/W)	0.067	0.061	0.059	0.056	0.047	N/A
		Comments	Thermal resistance decreases with increasing heat input, but slope of decrease is less than that of the vertical.					
	Horizontal	Comments	Thermosyphon is not able to transfer heat when horizontal. Heat input is initially set to 100 W. The temperatures near the evaporator increased very quickly while the remainder of the temperatures around the loop remained relatively constant. The heat input needed to be shut off, so the experiment did not reach the maximum temperature. Steady state was not reached.					
	Vertical (evaporator above condenser)	Comments	Thermosyphon is not able to transfer heat when oriented vertically with evaporator above condenser. Similar phenomenon is seen as in the horizontal orientation, except the temperature increase is steeper in the anti-gravity orientation.					
90%	Vertical (evaporator below condenser)	Single- or Two-phase?	Two-phase	Two-phase	Two-phase	Two-phase	Two-phase	Two-phase
		Pulsation?	No	Yes	Yes	Yes	Yes	Yes
		Vapor After Condenser?	No	No	No	No	No	No
		Operate as Heat Pipe?	TPLTS	TPLTS	TPLTS	TPLTS	TPLTS	TPLTS
		Thermal Resistance (K/W)	0.536	0.315	0.219	0.166	0.134	0.114
		Comments	N/A	N/A	N/A	N/A	N/A	N/A
	45° (evaporator below condenser)	Single- or Two-phase?	Two-phase	Two-phase	Two-phase	Two-phase	Two-phase	Two-phase
		Pulsation?	No	Yes	Yes	Yes	Yes	Yes
		Vapor After Condenser?	No	No	No	No	No	No
		Operate as Heat Pipe?	TPLTS	TPLTS	TPLTS	TPLTS	TPLTS	TPLTS
		Thermal Resistance (K/W)	0.516	0.321	0.231	0.177	0.145	0.118
		Comments	The thermal resistance for the angled experiment is approximately 3.6% less than the vertical experiment with a maximum percent difference occurring for the 300 W heat input.					
	Horizontal	Comments	Thermosyphon is not able to transfer heat when horizontal.Heat input is initially set to 100 W. The temperatures near the evaporator increased very quickly while the remainder of the temperatures around the loop remained relatively constant. The heat input needed to be shut off, so the experiment did not reach the maximum temperature. Steady state was not reached.					
	Vertical (evaporator above condenser)	Comments	Thermosyphon is not able to transfer heat when oriented vertically with evaporator above condenser. Similar phenomenon is seen as in the horizontal orientation, except the temperature increase is steeper in the anti-gravity orientation.					
75%	Vertical (evaporator below condenser)	Single- or Two-phase?	Two-phase	Two-phase	Two-phase	Two-phase	Two-phase	Two-phase
		Pulsation?	Yes	Yes	Yes	Yes	Yes	Yes
		Vapor After Condenser?	No	No	No	Yes	Yes	Yes
		Operate as Heat Pipe?	TPLTS	TPLTS	TPLTS	TPLTS	TPLTS	TPLTS
		Thermal Resistance (K/W)	0.349	0.204	0.139	0.115	0.100	0.075
		Comments	N/A	N/A	N/A	N/A	N/A	N/A
	45° (evaporator below condenser)	Single- or Two-phase?	Two-phase	Two-phase	Two-phase	Two-phase	Two-phase	Two-phase
		Pulsation?	No	Yes	Yes	Yes	Yes	Yes
		Vapor After Condenser?	No	No	No	No	No	No
		Operate as Heat Pipe?	TPLTS	TPLTS	TPLTS	TPLTS	TPLTS	TPLTS
		Thermal Resistance (K/W)	0.234	0.133	0.097	0.097	0.091	0.086
		Comments	For heat inputs of 300 W or less, the thermal resistance for the vertical orientation is higher than the 45° orientation. When the heat input is 350 W, the thermal resistance is lower in the vertical orientation than the 45° orientation. As heat input increases from 100–350 W, the percent difference in thermal resistance decreases from 39% at 100 W to −14% at 350 W.					
	Horizontal	Single- or Two-phase? Pulsation? Vapor After Condenser? Operate as Heat Pipe? Thermal Resistance (K/W) Comments	Thermosyphon is not able to transfer heat when horizontal.Heat input is initially set to 100 W. The temperatures near the evaporator increased very quickly while the remainder of the temperatures around the loop remained relatively constant. The heat input needed to be shut off, so the experiment did not reach the maximum temperature. Steady state was not reached.					
	Vertical (evaporator above condenser)	Single- or Two-phase? Pulsation? Vapor After Condenser? Operate as Heat Pipe? Thermal Resistance (K/W) Comments	Thermosyphon is not able to transfer heat when oriented vertically with evaporator above condenser. Similar phenomenon is seen as in the horizontal orientation, except the temperature increase is steeper in the anti-gravity orientation.					

For heat inputs of 100–300 W, the 45° orientation has a lower thermal resistance and is therefore more effective. However, for a heat input of 350 W, the opposite is true. The thermal resistance for the vertical orientation is less than that of the 45° orientation.

Based on results shown Fig. 20 and Table 5, the optimal orientation depends on heat input. For higher heat inputs, the vertical orientation is more effective and for lower heat inputs the 45° orientation is more effective. The heat input at which the transition occurs depends on fill ratio.

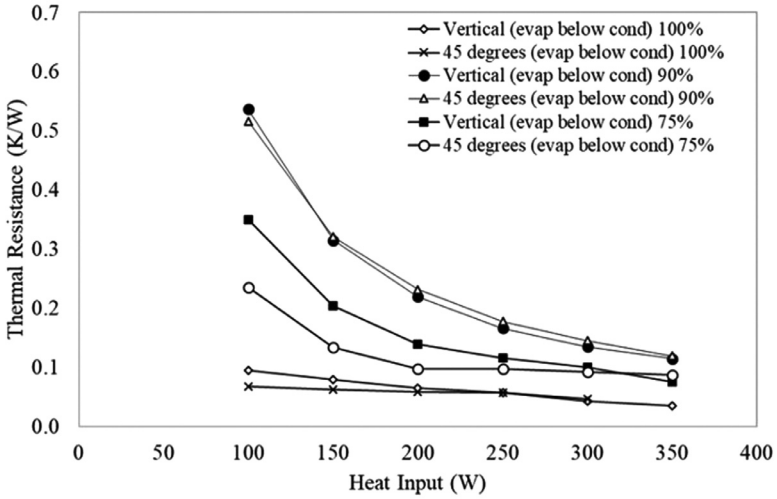

Fig. 20. Thermal resistance for 100%, 90%, and 75% water fill ratio loop thermosyphons with heat inputs from 100–350 W in the vertical and 45° orientation.

4.3. Comparison of effects of changing inclination angle between working fluids

The optimal orientation depends on different factors for water and R134a. When the working fluid is water, the thermosyphon has a lower thermal resistance in the 45° orientation for lower heat inputs, and in the vertical orientation for higher heat inputs. Therefore, the optimal orientation with water as the working fluid depends on the desired amount of heat to be transferred. With R134a as the working fluid, the optimal orientation depends on fill ratio. Higher R134a fill ratios (90% and 75%) operate more effectively in the vertical orientation, with the evaporator below the condenser, and the lower fill ratio of 60% operates more effectively at the 45° orientation.

5. Conclusions

There are several limiting factors for each working fluid in terms of heat input and fill ratio. With R134a as the working fluid, the loop thermosyphon is not able to operate as a SPLTS. The loop thermosyphon can operate as a TPLTS for fill ratios between 95–30% of the total loop volume for heat inputs of at least 200 W. The thermal resistance ranges from 0.0165–0.0256 K/W. The experiments with the lowest thermal resistance, and therefore optimal, are the 75–80% and 40% fill ratio experiments.

With water as the working fluid, the loop thermosyphon can operate effectively for liquid fill ratios of 100–30% relative to the total volume of the loop for heat inputs up to 350 W as either a SPLTS or TPLTS depending on initial fill ratio. When the working fluid is water, the experiment operates most effectively with the lowest thermal resistances for the 100% and 40% fill ratio experiments. The optimal orientation angle depends on heat input.

The loop thermosyphon operates with lower thermal resistance when R134a is the working fluid than with water. However, when the working fluid is water the experiment can operate as a SPLTS and can reach steady state at higher heat inputs. Both have an optimal fill ratio above and below 50%. The optimal fill ratio greater than 50% is 75–80% for the R134a and 100% for water, and the optimal fill ratio below 50% for both water and R134a LTS is 40%. The optimal orientation angle depends on fill ratio for R134a as the working fluid and desired amount of heat to be transferred and fill ratio for water as the working fluid.

Author statement

None.

Declaration of Competing Interest

None.

Acknowledgment

This material is based upon work supported by the National Science Foundation under grant no. 1744118 to the University of Connecticut.

Supplementary materials

Supplementary material associated with this article can be found, in the online version, at doi:10.1016/j.ijheatmasstransfer.2020.119312.

References

[1] Beitelmal, M.H., & Patel, C.D. (2002). *Two-phase loop: compact thermosyphon.*
[2] T.L. Bergman, A. Faghri, Review and advances in heat pipe analysis and numerical simulation, in: Numerical Simulation of Heat Exchangers, CRC Press, 2017, pp. 173–212.
[3] S. Boothaisong, S. Rittidech, T. Chompookham, M. Thongmoon, Y. Ding, Y. Li, Three-dimensional transient mathematical model to predict the heat transfer rate of a heat pipe, Adv. Mech. Eng. (2015), doi:10.1177/1687814014567811.
[4] S.W. Chang, D.C. Lo, K.F. Chiang, C.Y. Lin, Sub-atmospheric boiling heat transfer and thermal performance of two-phase loop thermosyphon, Exp. Therm. Fluid Sci. 39 (2012) 134–147, doi:10.1016/J.EXPTHERMFLUSCI.2012.01.017.
[5] A.A. Chehade, H. Louahlia-Gualous, S. Le Masson, I. Victor, N. Abouzahab-Damaj, Experimental investigation of thermosyphon loop thermal performance, Energy Convers. Manage. 84 (2014) 671–680, doi:10.1016/J.ENCONMAN.2014.04.092.
[6] R.T. Dobson, J.C. Ruppersberg, Flow and heat transfer in a closed loop thermosyphon. Part I – theoretical simulation, J. Energy South. Afr. 18 (3) (2007) 32–40.
[7] A. Faghri, Review and advances in heat pipe science and technology, J. Heat Transf. 134 (12) (2012) 123001, doi:10.1115/1.4007407.
[8] A. Faghri, Heat pipes: review, opportunites and challenges, Front. Heat Pipes (FHP) 5 (2014) 1, doi:10.5098/fhp.5.1.
[9] A. Faghri, Heat Pipe Science and Technology, 2nd ed., Global Digital Press, 2016.
[10] A. Faghri, Heat pipes and thermosyphons, in: Handbook of Thermal Science and Engineering, 2017, pp. 1–50, doi:10.1007/978-3-319-26695-4_52.
[11] A. Franco, S. Filippeschi, A. Franco, S. Filippeschi, S. Filippeschi, Closed loop two-phase thermosyphon of small dimensions: a review of the experimental results, Microgravity Sci. Technol. 24 (2012) 165–179, doi:10.1007/s12217-011-9281-6.

[12] W. Fu, X. Li, X. Wu, Z. Zhang, Investigation of a long term passive cooling system using two-phase thermosyphon loops for the nuclear reactor spent fuel pool, Ann. Nucl. Energy 85 (2015) 346–356, doi:10.1016/J.ANUCENE.2015.05.026.
[13] Kang, S.-W., Tsai, M.-C., Hsieh, C.-S., & Chen, J.-Y. (2010). *Thermal performance of a loop thermosyphon*.
[14] R. Khodabandeh, Pressure drop in riser and evaporator in an advanced two-phase thermosyphon loop, Int. J. Refrig. 28 (5) (2005) 725–734, doi:10.1016/J.IJREFRIG.2004.12.003.
[15] S. Kloczko, A. Faghri, Y. Li, Is a non-phase change heat pipe a new heat pipe, Int. J. Heat Mass Transf. 145 (2019), doi:10.1016/j.ijheatmasstransfer.2019.118676.
[16] S. Lee, D. Yuan, B. Wu, Experimental study on non phase change heat pipe and its mechanism analysis, in: 20th Nationalal and 9th International ISHMT-ASME Heat and Mass Transfer Conference, 2010, pp. 1624–1630, doi:10.3850/9789810838133.
[17] S. Lee, D. Yuan, B. Wu, Experimental study on the counter-gravity effect of non-phase change heat pipes, in: Proceedings of the 14th International Heat Transfer Conference, 2010, pp. 1–7.
[18] D. Lu, X. Zhang, C. Guo, Stability analysis for single-phase liquid metal rectangular natural circulation loops, Ann. Nucl. Energy 73 (2014) 189–199, doi:10.1016/J.ANUCENE.2014.06.014.
[19] M. Maiani, W.J.M. de Kruijf, W. Ambrosini, An analytical model for the determination of stability boundaries in a natural circulation single-phase thermosyphon loop, Int. J. Heat Fluid Flow 24 (6) (2003) 853–863, doi:10.1016/J.IJHEATFLUIDFLOW.2003.07.002.
[20] Y. Naresh, C. Balaji, Thermal performance of an internally finned two phase closed thermosyphon with refrigerant R134a: a combined experimental and numerical study, Int. J. Therm. Sci. 126 (2018) 281–293, doi:10.1016/J.IJTHERMALSCI.2017.11.033.
[21] K. Naveen, K.N. Iyer, J.B. Doshi, P.K. Vijayan, Investigations on single-phase natural circulation loop dynamics. Part 3: role of expansion tank, Prog. Nucl. Energy 78 (2015) 65–79, doi:10.1016/J.PNUCENE.2014.08.007.
[22] Y.J. Park, H.K. Kang, C.J. Kim, Heat transfer characteristics of a two-phase closed thermosyphon to the fill charge ratio, Int. J. Heat Mass Transf. 45 (23) (2002) 4655–4661, doi:10.1016/S0017-9310(02)00169-2.
[23] D.S. Pilkhwal, W. Ambrosini, N. Forgione, P.K. Vijayan, D. Saha, J.C. Ferreri, Analysis of the unstable behaviour of a single-phase natural circulation loop with one-dimensional and computational fluid-dynamic models, Ann. Nucl. Energy 34 (5) (2007) 339–355, doi:10.1016/J.ANUCENE.2007.01.012.
[24] L.M. Poplaski, A. Faghri, T.L. Bergman, Analysis of internal and external thermal resistances of heat pipes including fins using a three-dimensional numerical simulation, Int. J. Heat Mass Transf. 102 (2016) 455–469, doi:10.1016/j.ijheatmasstransfer.2016.05.116.
[25] Z. Tong, X.-H. Liu, Z. Li, Y. Jiang, Experimental study on the effect of fill ratio on an R744 two-phase thermosyphon loop, Appl. Therm. Eng. 99 (2016) 302–312, doi:10.1016/J.APPLTHERMALENG.2016.01.065.
[26] P.K. Vijayan, Experimental observations on the general trends of the steady state and stability behaviour of single-phase natural circulation loops, Nucl. Eng. Des. 215 (1–2) (2002) 139–152, doi:10.1016/S0029-5493(02)00047-X.
[27] P. Zhang, B. Wang, W. Shi, X. Li, Experimental investigation on two-phase thermosyphon loop with partially liquid-filled downcomer, Appl. Energy 160 (2015) 10–17, doi:10.1016/J.APENERGY.2015.09.033.